MIKE
Powered by DHI

MOUSE

Pollution Transport

Reference Manual

PLEASE NOTE

MOUSE POLLUTION TRANSPORT

Reference Manual - Surface Runoff Quality

1 The Build-up/Wash-off of Sediments

1.1 Accumulation of Particles on the Catchment

During dry weather periods sediments accumulate on the surface of urban catchments. The most common formulations of this process are to assume that the build up is a linear or an exponential function of time. Both formulations have been implemented in the model. The choice between the two formulations is not straightforward, due to insufficient experimental results.

The linear build up function is given as:

$$\begin{aligned} \frac{dM}{dt} &= A_c \qquad for \qquad M < M_{max} \\ \frac{dM}{dt} &= 0 \qquad for \qquad M \geq M_{max} \end{aligned} \tag{1.1}$$

where:

M	=	the accumulated mass of particles at time t (kg),
M_{max}	=	the maximum accumulated mass of particles on the catchment (kg),
t	=	the time in days,
A_c	=	the daily accumulation rate (kg/ha/day).

The exponential build up function is given as:

$$\frac{dM}{dt} = A_c - D_{rem} \cdot M \tag{1.2}$$

where:

M	=	the accumulated mass of particles at time t (kg),
t	=	the time in days,
A_c	=	the daily accumulation rate (kg/ha/day),
D_{rem}	=	the removal coefficient (*d-1*).

The coefficient D_{rem} represents the removal of particles from the surface by various mechanisms (e.g by wind, traffic, street sweeping, biological and chemical degradation) - all except wash off. The accumulated mass M will increase until a limit A_c/D_{rem} is reached.

An example of the two build up formulations is shown in Figure 1.

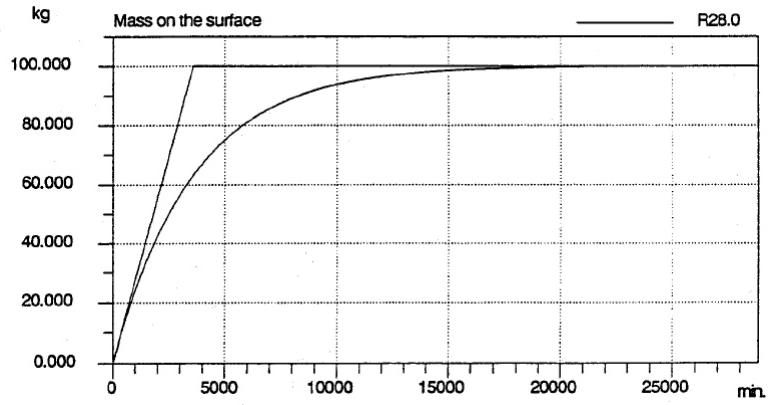

Figure 1.1 The linear and the exponential build up function. Maximum value = 100 kg and Build up rate = 40 kg/ha/day

1.2 Wash Off of Particles by Rainfall

Wash off of sediment particles during a rain event can be divided into two processes: erosion by raindrops and erosion by overland flow. Only the erosion by raindrops is taken into account in the model. Erosion by raindrops is governed by several parameters. The most important are: rainfall intensity, rainfall depth, rainfall duration, raindrop size, catchment topography, particle characteristics and vegetation. However, parameters such as raindrop size and rainfall depth are rarely available so a simpler approximation has been adopted in the model. This approximation states that the rain drop erosion is a function of the rain intensity and a detachment rate. The equation for the detachment by rainfall can be written as, (Ref. /1/):

$$V_{sr} = D_r\left(\frac{i_r}{i_d}\right)^{exp} LW(1-\varepsilon)A_s \qquad (1.3)$$

where:

V_{sr}	=	sediment volume detached by the rain per unit of time (m^3/h),
D_r	=	detachment coefficient for rainfall (m/h),
i_r	=	rainfall intensity (mm/h),
i_d	=	rain intensity constant (=25.4 mm/h),
exp	=	exponent (default value 2),
L	=	length of the catchment (m),
W	=	width of the catchment (m),
ε	=	porosity of the sediment,
A_s	=	fraction of surface area covered with sediment.

It is important to note that the erosion rate is independent of the diameter of the particles, hence the transport of the fine fraction is independent of the particle diameter. The transport of the coarse sediment is limited by the transport capacity of the overland flow, whilst the transport of the fine sediment only is limited by the rain erosion rate and the mass available on the surface. The transport capacity for the coarse fraction is calculated as the sum of the bed load and the suspended load transport capacity. The transport capacity for bed load and suspended load is calculated from the van Rijn formula (see the sediment transport reference manual).

2 The Sediment and Attached Pollutants

The description of the attachment of pollutants to sediment is based on the PPC concept, as described in the water quality reference manual. The mass attached to each fraction is determined as:

$$M_{fine} = TP \cdot S_{fine} \cdot FL$$
$$M_{coarse} = TP \cdot S_{coarse} \cdot CL \quad (2.1)$$

where:

TP	=	the pollutant in grams per litre wet sediment
M_{fine}	=	the load of pollutants attached to the fine sediment fraction(kg/s),
M_{coarse}	=	the mass of pollutant attached to the coarse sediment fraction (kg/s),
S_{fine}	=	the sediment transport of the fine fraction (m^3/s),
S_{coarse}	=	the sediment transport of the coarse fraction (m^3/s),
FL	=	the percentage of the total pollutant load (TP) attached to the fine fraction,
CL	=	the percentage of the total pollutant load (TP) attached to the coarse fraction.

3 The Gully Pots

3.1 The Processes in Gully Pots

The purpose of a gully pot is to trap particles and prevent them from entering the pipe system. Also, it prevents the release of odour from the pipe system. A sketch of a gully pot is shown in Figure 2.

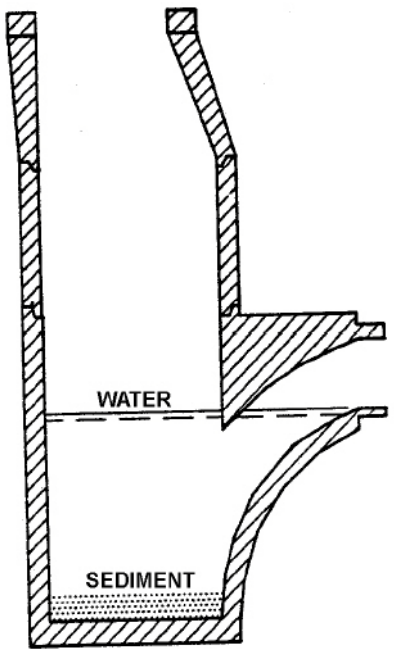

Figure 3.1 Sketch of a gully pot

The gully pot acts as a sediment trap during dry weather flow. During storms either deposition or erosion of sediment will take place depending on the flow conditions in the gully pot. Whether sediment will deposit or erode during storms depends on many different factors e.g.: the geometry of the gully pot, the depth of sediment in the gully pot, the level of turbulence in the gully pot and the sediment size and density. Furthermore, the removal of sediment from the gully pot by cleansing is an unknown factor.

Dissolved pollutants will build up in the gully pot liquid during dry weather. The build up is dependent on the type of pollutant, the biological/chemical conditions in the gully pot and the temperature.

3.2 Transport of Particles Through the Gully Pots to the Sewer System

During storms, the volume of liquid and sediment will remain unchanged in the gully pots. Thus, it is assumed that all sediment, which enters the gully pot is transported straight through the gully pot. This assumption is a necessary simplification, since the efficiency of trapping of sediment depends to a large degree on the local conditions in the gully pot. The amount trapped in the gully pot can be represented by a reduced detachment coefficient for rainfall or, for the fine fraction, by reducing the volume of sediment available on the surface.

3.3 The Build-up and the Release of Dissolved Pollutants in Gully Pots

The build-up of pollutants in the gully pot is assumed to be a linear function with a threshold value for the maximum concentration. The release of the polluted water during storm events is assumed to be a simple mixing process of the incoming water with the gully pot liquor as follows:

$$c_{out} = \frac{q_i \cdot c_i \cdot dt + V_{gully} \cdot c_{gully}}{V_{gully} + q_i \cdot dt} \tag{3.1}$$

where:

c_i	=	the concentration of pollutants in the inflow water,
c_{gully}	=	the concentration of pollutants in the gully pot,
c_{out}	=	the concentration of pollutants in the outflow water,
dt	=	the time step,
q_i	=	the inflow discharge,
V_{gully}	=	the volume of the gully pot.

4 Nomenclature

A_c daily accumulation rate (kg/ha/day)

A_s surface area fraction covered with sediment

CL percentage of the total pollutant load (*TP*) attached to the coarse sediment fraction

D_r detachment coefficient for rainfall

D_{rem} removal coefficient (d^{-1})

FL percentage of the total pollutant load (*TP*) attached to the fine sediment fraction

i_r rainfall intensity (mm/h)

i_d rain intensity constant (= 25.4 mm/h)

L length of the catchment (m)

M accumulated mass of particles at time t (kg)

M_{coarse} mass of pollutant attached to the coarse fraction

M_{fine} mass of pollutants attached to the fine fraction

M_{max} maximum accumulated mass of particles on the catchment

S_{coarse} sediment transport of the coarse fraction

S_{fine} sediment transport of the fine fraction

TP pollutant in grams per litre wet sediment

t time in days

V_{sr} sediment volume detached by the rain per unit of time (m³/h)

W width of the catchment (m)

e porosity of the sediment

5 References

/1/ Svensson, G., "Modelling of Solids and Metal Transport from small Urban Watersheds". Chalmers University of Technology, Göteborg, Sweden, 1987.

MOUSE POLLUTION TRANSPORT

Reference Manual - Sediment Transport

6 Introduction

Transport of sediments under impact of water in movement is a very complex process, which is impossible to be described in fully exact way. The reason is, among others, that the term "sediment" includes a very wide range of particles, which differ in size, shape and other physical properties. E.g. particle sizes may range from microscopic dimensions to boulders. The phenomena like graded sediment composition, sediment cohesion, bed forms, bed armouring, sedimentation, re-suspension, etc. and their importance for the sediment transport process have been intensively studied, resulting in numerous, semi-empirical or empirical sediment transport formulations.

Common for all existing deterministic sediment transport formulations is a relatively high level of uncertainty. The computed sediment transport may in some cases perfectly fit with the observations, while in some other case the two-fold error is not taken as a surprise. Therefore, when studying sediment transport, a sensible approach to the interpretation of the results must be taken.

Studying the sediment transport in sewers does not make the situation any easier. The actual physical conditions in sewer networks are far from the laboratory models. Also, the nature of the sewage-borne sediments is far away from an idealised sediment picture, containing even wider spectrum of particles than in natural streams.

The MOUSE ST module is a tool which attempts to provide a platform for deterministic modelling of sediments in sewer systems. Taken the previous discussion, the MOUSE ST users must apply this tool with due care and with full understanding of the underlying assumptions. Particularly, the risk of incorrect conclusions based on the "blind" interpretation of the results, must be considered and minimised.

The purpose of this Technical Reference manual is to describe the theory behind the MOUSE ST module. The manual describes the theories on a level which assumes that the user is familiar with the sediment transport terminology and only the main equations and assumptions from the various theories are presented here. For a complete back-ground on the theories please refer to the original references.

7 Non-Cohesive Sediment Transport - Sediment Properties

7.1 Particle Size

A qualitatively description of the particles size is given below:

Table 7.1

Material	Particle size [mm]
clay	< 0.002
silt	0.002 - 0.060
sand	0.060 - 2.000
gravel	2.000 - 64.000
cobbles/boulders	> 64.000

Particle size distribution can be established from a sieve analysis. The diameter obtained from the sieve analysis is termed the sieve diameter, d_s. The sieve analysis gives the frequency curve and the grain size distribution curve. Examples of the frequency curve and the grain size distribution curve are given in Figure 7.1 below:

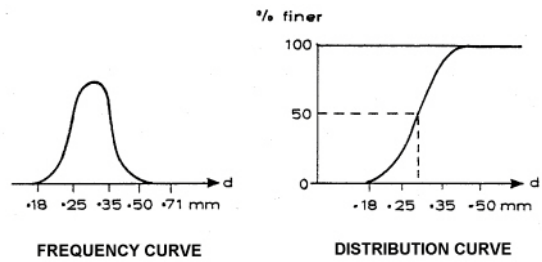

Figure 7.1 The grain size frequency and distribution curves

The percentile particle diameters (e.g. d_{35}, d_{50}, d_{65} and d_{90}) can be read of the grain size distribution curve.

Other two grain diameter size descriptors are often used in sediment transport analysis:

The spherical diameter, d_v - defined as the diameter of a sphere having the same volume as the given particle.

The fall diameter, d_f - defined as the diameter of a sphere having the same fall velocity in water at 24 °C.

The difference between d_s, d_v and d_f is usually less that 10 %. When a reference is made to the grain diameter in MOUSE ST, it is always the fall diameter of the particle.

7.2 The Porosity of Sediment

Sediment deposits consist of both solid particles and water contained in the spaces between the particles. The porosity is the ratio of void space in a volume to the total volume. The porosity is by definition:

$$\varepsilon = \frac{e}{1+e} \tag{7.1}$$

where

e = the void ratio.

7.3 The Fall Velocity

The sediment transport and the mode of the sediment transport is strongly dependent on the fall velocity (the settling velocity) of the particles in transport. The fall velocity is the terminal velocity of a particle settling in fluid under the action of gravity. The terminal velocity is attained when the gravity force and the drag force on the particle are in equilibrium. The equilibrium conditions are given in Equation (7.2), where the left hand side represent the gravity force and the right hand side the drag force.

$$(\gamma_s - \gamma)\frac{\pi}{6}d^3 = \tfrac{1}{2}c_D \rho w^2 \frac{\pi}{4}d^2 \tag{7.2}$$

where:

γ = specific weight of water (kg/(ms)^2),
γ_s = specific weight of sand (kg/(ms)^2),
d = the grain diameter (m),
c_D = the drag coefficient,
w = the settling velocity (m/s),
ρ = the density of water (kg/m3).

Rearranging equation (7.2) gives:

$$w = \sqrt{\frac{4(s-1)gd}{3c_D}} \tag{7.3}$$

where:

s = the specific gravity of the sediment grains (γ_s/γ),
g = the acceleration of gravity (m/s^2).

For a single spherical particle the drag coefficient, c_D, depends on the Reynolds number, Re, defined as:

$$Re = \frac{wd}{v} \tag{7.4}$$

The drag force can for small values of the Reynolds numbers be approximated by use of Stokes' Law:

$$F_D = 3\pi\mu dw \tag{7.5}$$

where F_D is the drag force (N).

Applying Stokes' Law the drag coefficient can be expressed as:

$$c_D = \frac{24}{Re} \tag{7.6}$$

This gives an expression for the settling velocity applicable for small particle sizes:

$$w = \frac{(s-1)gd^2}{18v} \tag{7.7}$$

The common expressions for the fall velocity of a solitary sand particle in a still, clear fluid are:

Particles in the range 0 - 100 µm, (Stokes 1851):

$$w_s = \frac{(s-1)gd^2}{18v} \tag{7.8}$$

Particles in the range 100 - 1000 µm (Zanke 1977):

$$w_s = \frac{10v}{d}\left[\left(1 + \frac{0.01(s-1)gd^3}{v^2}\right)^{0.5} - 1\right] \tag{7.9}$$

Particles larger than 1000 µm (van Rijn 1982):

$$w_s = 1.1[(s-1)gd]^{0.5} \quad (7.10)$$

Experiments have shown that for high sediment concentrations the fall velocity of the particles will be reduced due to hindered settling. An expression for the fall velocity for particles in the range 50-500 µm is given by Richardson-Zaki as:

$$w_{sh} = (1-c)^4 w_s \quad (7.11)$$

where w_{sh} is the fall velocity due to the hindered settling of the particles (m/s).

7.4 The Critical Bed Shear Stress

The critical bed shear stress is a concept used to describe whether the sediment motion will occur or not. The concept of the critical bed shear stress for a bed composed of uniform non-cohesive grains was put forward by Shields in 1936.

7.4.1 The Critical Bed Shear Stress on a Horizontal Bed

Shields' analysis was based on dimensional analysis. It is assumed that a particle would start to move for a given ratio between the driving forces and the stabilising forces. The driving forces acting on a sediment particle resting on a plane bed are the drag force, F_D, and the lift force, F_L. The drag force is given by:

$$F_D = \tfrac{1}{2} c_D \rho v^2 d^2 \quad (7.12)$$

and the lift force, F_L is proportional to the bed shear stress:

$$F_L \sim \tau d^2 \quad (7.13)$$

The stabilising forces on a sediment particle resting on a plane bed are the gravity force, F_G, and the frictional force, F_F. Both the stabilising forces are proportional to:

$$F_F, F_G \sim (\gamma_s - \gamma) d^3 \quad (7.14)$$

Shields introduced a parameter θ to represent the ratio between the driving and the stabilising forces:

$$\theta = \frac{F_D + F_L}{F_G + F_F} = \frac{\tau}{\gamma(s-1)d} = \frac{YI}{(s-1)d} = \frac{u_f^2}{(s-1)gd} \tag{7.15}$$

where θ is the dimensionless bed shear stress or the Shields parameter.

The sediment grains start to move when the dimensionless bed shear stress θ exceeds the critical bed shear stress θ_c. The critical bed shear stress was found to be a function of the grain Reynolds number:

$$Re = \frac{u_f d}{v} \tag{7.16}$$

For large values of the Reynolds number it was found that $\theta_c \approx 0.06$.

An approximation to the critical bed shear stress, θ_c, was given by van Rijn (1984). Van Rijn defined a curve describing the Shields curve for the critical bed shear stress as a function of the particle number, D_*. The particle number is defined as:

$$D_* = \left(\frac{(s-1)g}{v^2}\right)^{1/3} d_{50} \tag{7.17}$$

The relationships describing van Rijn's curve are given below:

Table 7.2

$D_* \leq 4$	$\theta_c = 0.24\ (D_*)^{-1.00}$
$4 < D_* \leq 10$	$\theta_c = 0.14\ (D_*)^{-0.64}$
$10 < D_* \leq 20$	$\theta_c = 0.04\ (D_*)^{-0.10}$
$20 < D_* \leq 150$	$\theta_c = 0.013\ (D_*)^{0.29}$
$150 < D_*$	$\theta_c = 0.055$

These relationships for the critical bed shear stress on a horizontal bed are shown in Figure 7.2.

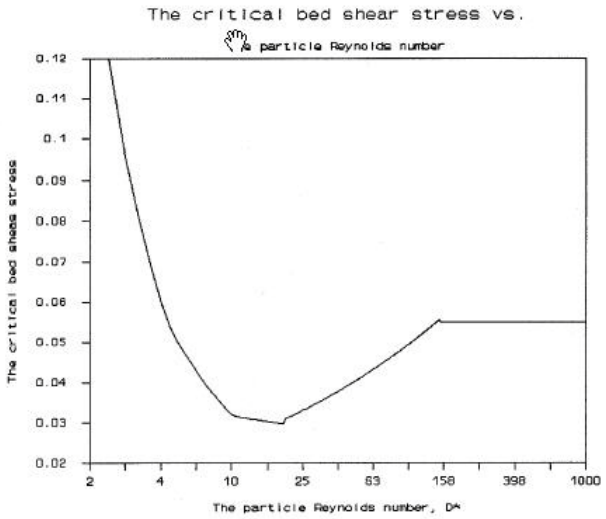

Figure 7.2 Van Rijn's relationships for the critical bed shear stress based on the particle number

8 Flow Resistance in Sewers with Sediment Deposits

The calculation of the flow resistance is far more complex for sewers with sediment deposits than for the clean sewers. This is because the hydraulic resistance in the sewer originates partially from the pipe wall, while another part originates from the sediment on the bottom of the sewer. Further, the resistance from the sediment deposits consists of two contributions. One part originates from the grain friction and the other part originates from the expansion loss behind the bed forms. The configuration of the bed forms is determined by the sediment transport and the flow.

In summary, the principal sources of roughness in sewers are:

- Resistance from the pipe material itself,
- Resistance from the sediment grains,
- Resistance from bed forms in the conduit,
- Other factors: aging effects, structural failure, biological growth.

The resistance from the pipe and the resistance from the sand grains themselves can be described through common hydraulic theory. The resistance from the bed forms can be described through sediment transport formulae. The sediment transport formulae are described in the next paragraph. The description of the resistance from the other factors such as: aging effects, structural failure and biological growth out is not included in MOUSE ST.

8.1 The Resistance from Bed Forms

The surface of sediments deposited in a sewer where sediment transport occurs will take one of the following bed forms (see the illustration in Figure 8.1:

- Ripples,
- Dunes,
- Plane bed,
- Anti-dunes (standing waves - chute and pool).

A short characterization of the different bed forms is given below. The bed forms, which occur in sewers are ripples, dunes and plane bed. Anti-dunes are not likely to occur in sewer systems as the sediment bed will be totally eroded during the previous flow stages.

Ripples

Ripples are triangular sand waves with a small wavelength (compared to the water depth). Ripples are usually formed in fine sediments at rather low transport rates. Ripples are therefore often associated with hydraulically smooth beds.

Dunes

Dunes are large, triangular sand waves and they are long compared to their height. Dunes are generally irregular and three-dimensional. Coarse sediments normally form dunes.

Both ripples and dunes have a gently curved upstream side and a steep downstream side with a slope close to the angle of repose (approx 27°). At the crest of the bed forms the flow separates and a bottom roller is formed. The formation of ripples and dunes on an originally plane bed has been explained through stability analyses (e.g. Engelund, 1970). Small sinusoidal perturbations of the bed are found to increase with time and the wavelength with the highest amplitude corresponds to the wavelength of the emerging bed waves.

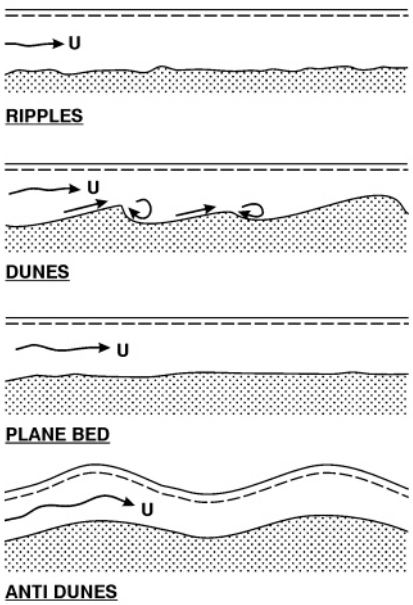

Figure 8.1 Development of bed forms for increasing flow velocity

Plane Bed

Stability analyses have shown that in the case of a high level of suspended load, a plane bed will remain stable. This is due to the time lag between the local hydraulic conditions and the suspended load.

Anti-dunes

Anti-dunes appear when the perturbation of the water surface is in phase with the bed perturbations. This occurs when the Froude number, *F*, exceeds the limit for supercritical flow:

$$F > \sqrt{\frac{\tanh(k \cdot Y)}{k \cdot Y}} \qquad (8.1)$$

where:

k = the wave number of the bed forms,
Y = the water depth.

Anti-dunes are nearly sinusoidal bed waves, which generally move upstream. The water surface is also sinusoidal, in phase with the bed waves and with larger amplitude. The anti-dunes may vary in a cyclic manner, growing until breaking of the surface wave occurs, then being washed out before new small ones are formed which then start to grow again. As anti-dunes only occur when the Froude number is high and when a free water surface is present, anti-dunes are not likely to occur in sewer systems.

The variation of the bed shear stress with the velocity is shown in Figure 8.2. τ' is the skin friction, the friction if the bed had stayed plane. τ'' is the form friction, the extra resistance to the flow due to bed forms.

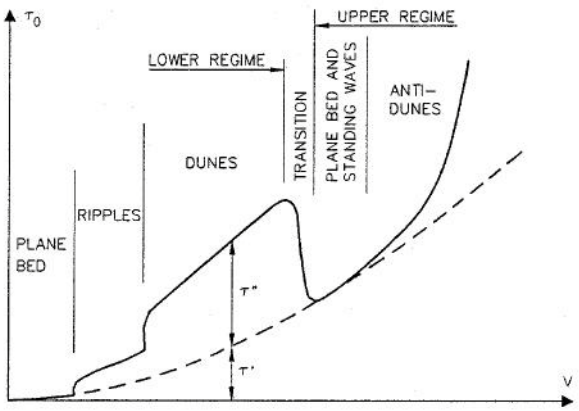

Figure 8.2 Variation in bed shear stress for increasing flow velocity

8.2 Description of the Shear Stress in Sewers

Description of the flow in a pipe with a sediment bed is complicated by the fact that the shear stress from the pipe wall and the sediment bed differs. A side wall elimination procedure can be used to describe the total resistance to the flow when the hydraulic conditions and the characteristics of the sediment layer are known.

8.2.1 The Einstein Side Wall Elimination Procedure

The side wall elimination is based upon the findings by Einstein (1942) and Vanoni-Brooks (1957). The former uses the Mannings equation and the latter

the Darcy Weisbach's equation. MOUSE ST uses the Einstein side wall elimination procedure, according to the following description.

The basic assumptions of the Einstein side wall elimination procedure are:

- The cross-section area can be divided into different areas where each of the flow areas can be connected to a part of the wetted perimeter,
- The mean velocity is the same for the whole section,
- The hydraulic gradient is the same for the whole section.

Einstein used these assumptions to separate the resistance from the side walls and the bottom in channel flow. Gustavo Perrusquía (1986) has shown that this procedure is applicable to sewers as well. A definition sketch of a sewer with sediment is shown in Figure 8.3.

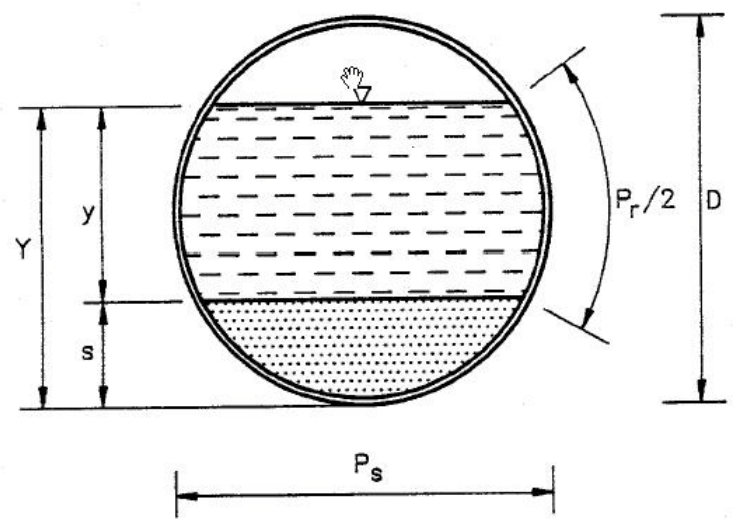

Figure 8.3 A definition sketch of a sewer with a sediment deposit

The side wall elimination procedure assumes the total flow resistance can be written as the sum of the resistance from the different parts of the flow:

$$F = P \cdot \tau = P_r \cdot \gamma \cdot R_r \cdot I_r + P_s \cdot \gamma \cdot R_s \cdot I_s \quad (8.2)$$

By use of the Manning equation:

$$V = n \cdot \sqrt{I} \cdot R^{2/3} \quad (8.3)$$

The slopes (I, I_r, I_s) can be eliminated from Equation (8.2)

$$P \cdot n^2 \cdot \frac{V^2}{R^{1/3}} = P_r \cdot n_r^2 \cdot \frac{V_r^2}{R_r^{1/3}} + P_s \cdot n_s^2 \cdot \frac{V_s^2}{R_s^{1/3}} \tag{8.4}$$

It is assumed the velocity varies with the hydraulic radius in the following way:

$$\frac{V}{R^{1/6}} = \frac{V_r}{R_r^{1/6}} = \frac{V_s}{R_s^{1/6}} \tag{8.5}$$

This gives:

$$n = \sqrt{\frac{P_r \cdot n_r^2 + P_s \cdot n_s^2}{P}} \tag{8.6}$$

where:

P_r	=	the wetted perimeter of the pipe wall,
P_s	=	the width of the sediment bed and P is the total wetted perimeter,
n_r	=	the Manning number for the pipe,
n_s	=	the Manning number for the bed,
n	=	the total resistance to the flow.

Equation (8.6) was suggested by Einstein 1950. It estimates the weighted resistance to the flow for a cross-section where the wall roughness differs from the bed roughness.

9 Non-Cohesive Sediment Transport Formulae

Four sediment transport models have been implemented in the MOUSE ST. These are: the Ackers-White Model, the Engelund-Fredsøe Model, the Engelund-Hansen Model and the van Rijn model. Further, it is possible to transport fine sediment by the use of the advection-dispersion equations. The Ackers-White and the Engelund-Hansen models calculate the total transport, while the Engelund-Fredsøe and the van Rijn models divide the sediment transport into bed load and suspended load. Furthermore, the Engelund-Fredsøe and the van Rijn models can simulate the development of sand dunes in pipes. The total bed resistance is calculated as the sum of a contribution from the skin friction acting on the dune and an expansion loss behind the dune.

The selection of a transport model for a particular application depends on the nature of the area under study, and on experience in sediment transport modelling. It is at present doubtful whether the models which calculates both bed load and the suspended load estimate the sediment transport better than the models which only calculate the total load.

9.1 The Modes of Sediment Transport

The sediment transport is usually split into three transport modes:

- Wash load,
- Bed load,
- Suspended load.

The mode of transport depends on the particle characteristics and the hydraulic conditions, i.e. particles which are transported as bed load during some flow conditions may be transported as suspended load during other flow conditions. A qualitative description of the three transport modes is given below.

9.1.1 The Wash Load Transport

The wash load consists of fine sediment transported predominantly in suspension. The exchange between the bed material and the wash load is in general small. The wash load has often a uniform vertical concentration distribution. Common sediment transport formulae do not include the transport of wash load. Instead, the transport of wash load can be described by the use of the advection-dispersion equations.

9.1.2 The Bed Load Transport

The bed load consists of those particles which move in almost continuous contact with the bed during the transport, e.g., by rolling, jumping or sliding.

9.1.3 The Suspended Load Transport

The suspended load is transported without continuously contact with the bed. A particle is transported as suspended load if the turbulence eddies have large vertical velocity components. In steady uniform flow the vertical distribution of sediment can be described by:

$$(1-c)cw+\varepsilon\frac{dc}{dy}=0 \tag{9.1}$$

where:

c	=	the concentration,
w	=	the fall velocity,
ε	=	the diffusion coefficient,
y	=	the height above the bed,

Equation (9.1) is a balance between the transport through a horizontal unit area, where $w \cdot c$ is the downward movement and $\varepsilon \cdot dc/dy$ is the upward diffusion of particles through the area.

9.2 The Diffusion Coefficient

The turbulent diffusion of fluid momentum is usually described by the use of a parabolic distribution, Equation (9.2). In order to achieve a better description of the concentration profile, some scientists (e.g. van Rijn) use a parabolic expression in the lower half part of the fluid and a constant diffusion coefficient in the upper half of the fluid. The parabolic-constant expression is given in Equation (9.3). Some others (e.g. Fredsøe and Deigaard) use a linear-constant relationship. The linear-constant relation is given in Equation (9.4).

$$\varepsilon = \frac{y}{Y}\left(1-\frac{y}{Y}\right)\kappa u_f Y \tag{9.2}$$

The van Rijn expression for the diffusion coefficient:

$$\begin{aligned}\varepsilon &= \frac{4y}{Y}\left(1-\frac{y}{Y}\right)\varepsilon_{max} \qquad for \qquad \frac{y}{Y}\le 0.5\\ \varepsilon_{max} &= 0.25\kappa u_f d \qquad for \qquad \frac{y}{Y}>0.5\end{aligned} \tag{9.3}$$

The Fredsøe and Deigaard expression for the diffusion coefficient:

$$\varepsilon = \kappa u_f y \qquad for \qquad 0 \le \frac{y}{Y} \le 0.192$$
$$\varepsilon = u_f Y / 13 \qquad for \qquad 0.192 \le \frac{y}{Y} \le 1 \tag{9.4}$$

10 The Ackers-White Model

The Ackers-White model consists of the sediment transport model presented by Ackers and White (1973) and an extension to the model for the description of the resistance developed White et al. (1979). The sediment transport model is described first, as the formulation of the resistance uses many of the variables defined for the sediment transport model.

10.1 The Ackers & White Sediment Transport Model

Ackers and White (1973) presented a semi-empirical sediment transport model. The model is partly based on dimensional analysis and partly on physical arguments. The steam power concept has been used to derive the form of the function that was tested.

Ackers and White assume coarse sediments to be transported, mainly as bed processes. The Ackers-White sediment transport model is expressed in a dimensionless form described in Equation (10.1). G_{gr} is the general transport parameter defined as:

$$G_{gr} = \frac{X \cdot Y}{s \cdot d}\left(\frac{U_f}{U}\right)^n \tag{10.1}$$

where X is the volumetric concentration of sediment transport as a mass flux per unit mass flow rate.

Ackers and White showed that G_{gr} can be written as a function of the variables F_{fg} and D_{gr} , i.e. $G_{gr} = f(F_{fg}, D_{gr})$. The expressions for F_{fg} and D_{gr} are given below.

$$G_{gr} = C\left(\frac{F_{gr}}{A} - 1\right)^m \tag{10.2}$$

in which C, m and A are model parameters depending on the dimensionless grain diameter D_{gr}, defined as:

$$D_{gr} = d\left[\frac{g(s-1)}{v^2}\right]^{1/3} \tag{10.3}$$

where:

d	=	grain size,
v	=	the kinematic viscosity,
s	=	the relative density of the sediment.

Note, D_{gr} is the same parameter as van Rijn has defined as the particle number D_*.

F_{gr} is the general sediment mobility number defined as:

$$F_{gr} = \frac{U_f^n}{\sqrt{gd(s-1)}} \cdot \left(\frac{U}{\sqrt{32}\log\left(\frac{10Y}{d}\right)} \right)^{1-n} \tag{10.4}$$

where:

U_f = the friction velocity,

Y = the water depth,

n = a model constant depending on D_{gr} and ranges from 0 to 1 (coarse material to fine material).

Inserting these values of n into Equation (10.4) gives the sediment mobility numbers for coarse (F_{cg}) and fine (F_{fg}) material, respectively:

$$F_{cg} = \frac{U}{\sqrt{32gd(s-1)}\log\left(\frac{10Y}{d}\right)} \tag{10.5}$$

$$F_{fg} = \frac{U_f}{\sqrt{gd(s-1)}} \tag{10.6}$$

In determining the model parameters, Ackers and White distinguished between three cases: fine grains, coarse grains and a transitional grain size. The classification is based on D_{gr}.

D_{gr}< 1 (Fine grains):

n = 1
A = 0.37
C = $2.95 \cdot 10^{-4}$
m = 11

$1 < D_{gr} < 60$ (Transitional grain size):

$n = 1.0 - 0.56 \log D_{gr}$

$$A = \frac{0.23}{\sqrt{D_{gr}}} + 0.14 \tag{10.7}$$

$$\log(C) = 2.86 \log D_{gr} - (\log D_{gr})^2 - 3.53 \tag{10.8}$$

$$m = \frac{9.66}{D_{gr}} + 1.34 \tag{10.9}$$

$D_{gr} > 60$ (Coarse grains):

$n = 0$
$A = 0.17$
$C = 0.025$
$m = 1.50$

The sediment transport rate can be determined directly as a function of D_{gr}, U_f, velocity and the water depth.

10.2 Flow Resistance - White et al.

The flow resistance model developed by White et al. (1979) is an extension to the Ackers-White sediment transport. The model is semi-empirical, i.e. the governing parameters are found by dimensional analysis and, from the analysis of a large amount of data, a functional relation has been determined.

White et al. suggest that the alluvial roughness is a function of the three dimensionless variables: D_{gr}, F_{gr} and F_{fg}.

D_{gr}, F_{gr} and F_{fg} are defined in the previous paragraph: The Ackers & White Sediment Transport Model *(p. 43)*.

Based on a large number of experimental data White et al. have found a functional relation of the form:

$$\frac{F_{gr} - A}{F_{fg} - A} = f(D_{gr}) \tag{10.10}$$

where A is the critical mobility number for initiation of motion, given as a function of D_{gr}.

The range of applicability for Equation (10.10) is:

$F < 0.8$ and $1 < D_{gr} < 60$.

Curve fitting suggested two different expressions for the right hand side of Equation (10.10), viz.

$$f(D_{gr}) = 1 - 0.76\left[1 - \frac{1}{\exp[(\log D_{gr})^{1.7}]}\right] \quad (10.11)$$

when D_{gr}, F_{gr} and F_{fg} are based on d_{35}, and

$$f(D_{gr}) = 1 - 0.70\left[1 - \frac{1}{\exp[(1.4\log D_{gr})^{2.65}]}\right] \quad (10.12)$$

when the parameters are based on d_{65}.

Testing the model on a set of independent data (both experimental and prototype data) White et al. found that Equation (10.11) gave slightly better results than Equation (10.12).

An iterative procedure is used to determine the alluvial roughness coefficient. The general sediment mobility number can be expressed in terms of the fine grain mobility as follows:

$$F_{gr} = (F_{fg})^n \cdot t \quad (10.13)$$

where t is a function of U, Y etc. but it is known:

$$T = \left[\frac{U}{\sqrt{32gd(s-1)}} \cdot \log\left(\frac{10Y}{d}\right)\right]^{1-n} \quad (10.14)$$

Inserting Equation (10.13) into Equation (10.10) yields:

$$F_{fg} = \frac{t}{f(d_{gr})} \cdot F_{fg}^n + \left(1 - \frac{1}{f(d_{gr})}\right)A \quad (10.15)$$

This formula can be used iteratively to calculate F_{fg} because both $t / f(D_{gr})$ and n are greater than 0 but smaller than 1. Subsequently, F_{fg} can be substituted into Equation (10.4) to obtain U_f. It is now possible, using Equations (10.6) and (10.12) under the heading Ackers and White Model, to solve the equations for the sediment transport rate.

11 The Engelund-Hansen Model

11.1 Flow Resistance - The θ - θ' Relation

When the bed is covered by bed forms, the total bed shear stress τ, can be divided into two parts, τ' and τ''.

τ' is the shear stress acting on the gently curved upstream surface of the dunes, named the skin friction and τ'' is caused by the form drag on the dunes. The total dimensionless bed shear stress θ, can then be written as:

$$\theta = \theta' + \theta'' \tag{11.1}$$

where:

$$\theta = \frac{\tau/\rho}{(s-1)gd}, \quad \theta' = \frac{\tau'/\rho}{(s-1)gd} \quad \textit{and} \quad \theta'' = \frac{\tau''/\rho}{(s-1)gd} \tag{11.2}$$

with:

ρ	=	the density of water,
s	=	the relative density of the bed material,
d	=	the mean grain size of the bed material,
g	=	the acceleration of gravity.

Engelund and Hansen (1966) found, by applying the principle of similarity, that a relationship exists between the dimensionless total bed shear stress θ, and the dimensionless skin friction θ', see Figure 11.1 and Figure 11.2. The relation for a dune-covered bed can be approximated by:

$$\theta' = \theta_c + 0.4\theta^2 \tag{11.3}$$

In the case of a plane bed, the form drag becomes zero and the relation reads:

$$\theta = \theta' \tag{11.4}$$

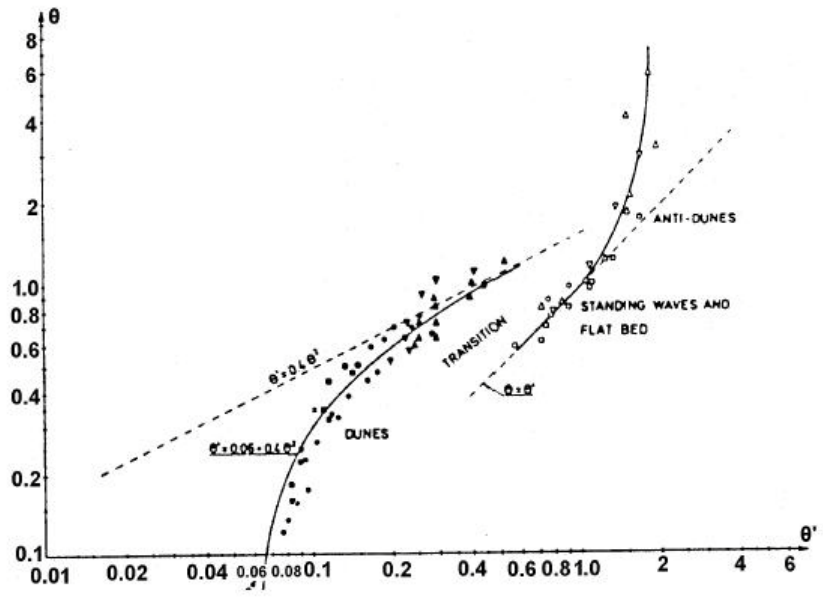

Figure 11.1 Plot of θ versus θ' (Experimental Data)

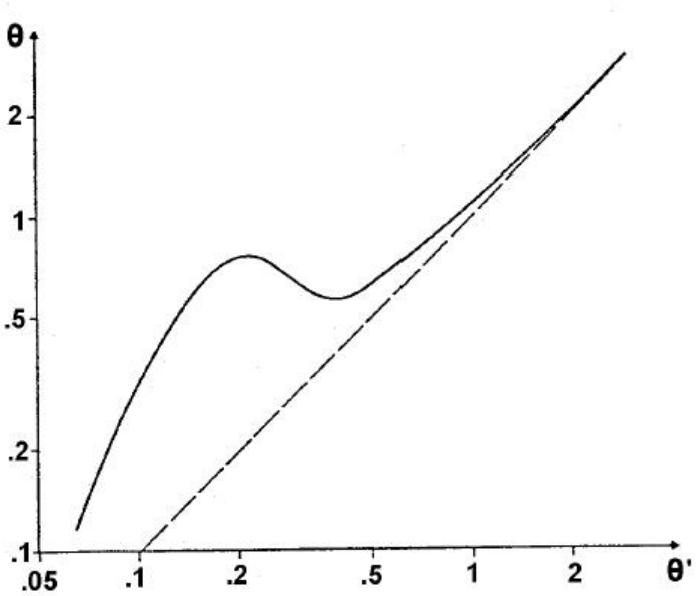

Figure 11.2 Plot of θ versu θ' (theoretical expression)

The flow over the 'smooth' upstream side of the dune can be de-scribed by the boundary layer equation:

$$\frac{U}{U_f'} = 2.5\left(\ln\left(\frac{30y'}{k_s}\right) - 1\right) \tag{11.5}$$

where:

$$U_f' = \sqrt{\frac{\tau'}{\rho}} \tag{11.6}$$

with:

U	=	the mean flow velocity,
y'	=	the boundary layer thickness, $y' = Y\,\theta'/\theta$, where Y= mean flow depth,
k_s	=	the equivalent sand roughness of the dune surface, $k_s \sim 2.5\,d$.

Under weak non-uniform flow conditions, the steady state flow conditions can thus be found as a function of the discharge and the depth by use of the fol-lowing four equations:

$$U_f' = \frac{U}{2.5\left(\ln\left(\frac{30y'}{k_s}\right) - 1\right)} \tag{11.7}$$

$$\theta' = U_f'^2/(s-1gd) \tag{11.8}$$

$$\theta = f(\theta') \tag{11.9}$$

$$y' = Y \cdot \theta'/\theta \tag{11.10}$$

Equations (10.11) and (11.7) to (11.10) can be solved by iteration.

The Manning or Chezy coefficient is calculated from the mean flow velocity, the depth and the total dimensionless bed shear stress:

$$\frac{g}{C^2} = \theta(s-1)gd\ \rho/U^2 \tag{11.11}$$

The relation between the Manning's *M* and the Chezy number is:

$$M = C \cdot R^{1/6} \tag{11.12}$$

11.2 Modifications to the θ - θ' Relation

The relation given in Equation (11.3) is found from observations of the nature. However, in the nature discontinuous rating curves are found. Hence, there exist two water levels for a given discharge, meaning that there are two solutions to Equation (11.3). This makes the equation unsuitable for a computer programme. Challet and Chunge (1980) proposed a modified $\theta - \theta$' relation without the disadvantages mentioned above. The modified relation is:

Table 11.1

$\theta \leq 0.06$	$\theta' = \theta$
$0.06 < \theta \leq 0.30$	$\theta' = 0.136 \cdot \theta^{0.292}$
$0.30 < \theta \leq 0.90$	$\theta' = 0.06 + 0.4 \cdot \theta^2$
$0.90 < \theta \leq 1.10$	$\theta' = 0.667 \cdot \theta^{5.24}$
$1.10 < \theta$	$\theta' = \theta$

This θ - θ' relation is used in the MOUSE Sediment Transport Model.

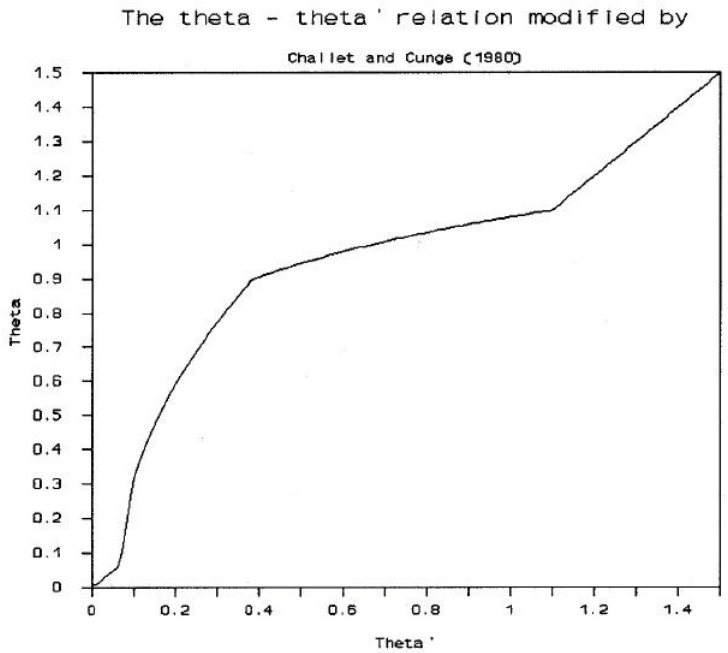

Figure 11.3 The $\theta - \theta$' relation modified by Challet and Cunge (1980)

11.3 The Engelund & Hansen Sediment Transport Model

Engelund and Hansen (1967) presented a sediment transport formula which is derived from considerations of the work done by the water flow on the sediment in transport. Although the formula was derived for a dune-covered bed, it was found to be applicable to the upper regime (plane bed and anti-dunes) as well.

The Engelund & Hansen transport equation reads:

$$\Phi = \frac{0.1}{f} \cdot \theta^{\frac{5}{2}} \tag{11.13}$$

where:

θ = the total dimensionless bed shear stress,
f = the friction factor, defined as $2\,Uf^2/U^2$ where Uf and U are the friction and current velocities respectively.
Φ = the dimensionless sediment transport defined as:

$$\Phi = \frac{q_t}{\sqrt{(s-1)gd^3}} \tag{11.14}$$

where q_t is the total bed material transport per unit width.

12 The Engelund & Fredsøe Model

The sediment transport model presented by Engelund & Fredsøe (1976) gives a more detailed description of the sediment transport and its relation to the flow resistance. The total sediment transport is split up into a calculation of the bed load and the suspended load. The sediment within a layer of two times the particle diameter is assumed to travel as bed load, which is the same approached as used by Einstein (1950). The sediment transport is calculated from the skin friction, i.e. the shear stress acting on the surface of the dunes.

If the sediment transport model is to be used to calculate the resistance to the flow from the dunes, it is necessary to distinguish between suspended load and bed load, in order to estimate the variation in the size of the dunes. When the resistance is calculated from the dunes, hysteresis effects from dunes can be simulated.

It is, at present, doubtful whether the models which split the sediment load into bed load and suspended load are more reliable in determining the total transport than the transport formulae which consider the sediment transport as a whole.

12.1 The Engelund & Fredsøe Sediment Transport Model

12.1.1 The Bed Load

The velocity of the particles moving as bed load has been found to be:

$$U_{bs} = 10U_f'\left(1 - \sqrt{1/2}\sqrt{\frac{\theta_c}{\theta}}\right) \tag{12.1}$$

where:

U_{bs} = the velocity of bed load particles,
U_f' = the friction velocity of the boundary layer,
θ = the dimensionless bed shear stress,
θ_c = the critical dimensionless bed shear stress.

The number of surface particles which move per unit area is p/d, where p is the probability for the particles to move:

$$p = \left\{1 + \left(\frac{\pi/6\ \beta}{\theta' - \theta_c}\right)^4\right\}^{-\frac{1}{4}} \tag{12.2}$$

with:

θ' = the dimensionless skin friction,
β = the dynamic friction coefficient approx. equal to 0.65.

The probability *p* has been determined so that for moderate θ values all of the bed shear stress τ, exceeding the critical value τ_c, is transferred to the bed through drag forces on the moving bed load particles. For high θ values the limiting value for *p* is 1. By combining Equations (12.1) and (12.2) Engelund & Fredsøe found the following bed load function:

$$\Phi_b = \left\{1 + \left(\frac{\pi/6\ \beta}{\theta' - \theta_c}\right)^4\right\}^{\frac{1}{4}} (\sqrt{\theta'} - \sqrt{1/2}\sqrt{\theta_c}) \tag{12.3}$$

12.1.2 The Suspended Load

The suspended load q_s, is found as the integral of the current velocity, *u(y)*, and the concentration of suspended sediment, *c(y)*:

$$q_s = \int_a^h c\ u\ dy \tag{12.4}$$

In the Equation (12.4), *a* is the thickness of the bed layer which can be approximated by $2 \cdot d_{50}$, where d_{50} is the mean grain diameter. The current velocity *u*, at a distance *y* above bed level is described by the logarithmic velocity profile:

$$u = 2.5 U'_f \ln\left(\frac{30y}{k_s}\right) \tag{12.5}$$

where U'_f is the boundary layer thickness and the equivalent sand roughness k_s is equal to 2.5 d_{50}.

The concentration is calculated in accordance with the concentration profile derived by Rouse (1937):

$$: = c_b\left(\frac{Y-y}{y}\frac{a}{Y-a}\right)^z \tag{12.6}$$

where:

Z = the Rouse number: $Z = w/(0.4 \cdot U_f)$,
c_b = the concentration at the bed,
w = the settling velocity of the suspended material (Equations (7.8) - (7.10)).

Only grains with a settling velocity smaller than 0.8 U_f can be carried in suspension and only these grains are considered in the calculation of the effective fall velocity. The grain-size distribution is assumed to have a logarithmic - normal distribution. The grain sizes not carried in suspension are subtracted from this distribution and the mean grain size of the remaining sediment is used in Equations (7.8) - (7.10).

The bed concentration, c_b, at a distance $y = 2 \cdot d$ from the bed, according to Engelund & Fredsøe, is determined through dynamic considerations: For increasing values of θ, the bed shear stress exceeding τ_c cannot be transferred by the drag on the bed load particles alone. A part of the bed shear stress is transferred as a dispersive stress, i.e. through collisions between suspended particles close to the bed. The dispersive stress is described by the expressions developed by Bagnold (1954).

Thus, the total non-dimensional bed shear stress θ' (corrected from the effect of dunes), is made up of three terms: the critical shear stress, the drag on bed load particles and the dispersive stress from the suspended load, defined as:

$$\theta' = \theta_c + \frac{\pi}{6}\beta p + 0.027 s \theta' \lambda_b^2 \tag{12.7}$$

where p is the probability of particles to move.

The linear concentration λ_b is related to c_b by:

$$c_b = \frac{0.65}{(1 + 1/\lambda_b)^3} \tag{12.8}$$

With known bed concentration c_b and settling velocity w the integral Equation (12.4) can be evaluated with, for instance, the use of the diagrams presented by Einstein (1950). The integral cannot be expressed in closed form and, during numerical simulations, it must be integrated numerically or an approximation must be applied.

12.2 The Engelund & Fredsøe Flow Resistance

If the dune dimensions (height and length) are known, the hydraulic resistance (bed shear stress) can be calculated from the water depth and the discharge. Furthermore, the portion of the dimensionless bed shear stress θ' which is acting as skin friction on the gently curved upstream side of the dunes can be determined.

The total bed shear stress τ, is as previously split up into the skin friction, τ', and the form friction τ'':

$$\tau = \tau' + \tau'' \tag{12.9}$$

t'' is mainly caused by the expansion loss behind each dune and is described as Carnot losses, (Engelund & Hansen 1967) :

$$\frac{\tau''}{\rho} \approx \frac{\alpha q^2 Y}{2L}\left(\frac{1}{Y} - \frac{1}{Y+H}\right)^2 \approx \frac{\alpha U^2 H^2}{2YL} \tag{12.10}$$

where:

H	=	the dune height,
L	=	the dune length,
α	=	the velocity distribution coefficient which is close to one,
U	=	the current velocity,
q	=	the discharge per unit width.

The total dimensionless shear stress θ, can thus be written as:

$$\frac{\tau}{(s-1)gd} = \theta = \theta' + \frac{\alpha U^2 H^2}{2(s-1)gdYL} \tag{12.11}$$

The Equation (12.11) is now used instead of Equation (11.9). The Equations (10.11), (11.7), (11.8), (12.11) and (11.10) and can be solved now within a few iterations.

12.2.1 The Equilibrium Dune Height

With the model presented by Fredsøe (1979) the equilibrium dune height can easily be found as a function of θ_{top} (the dimensionless shear stress taken at the dune top).

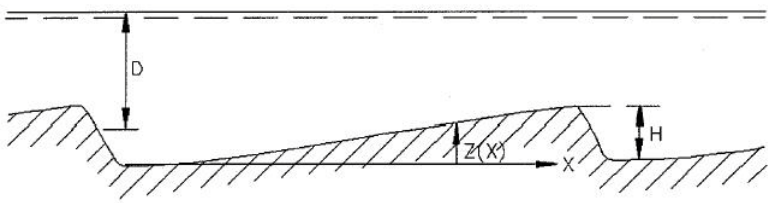

Figure 12.1 Sketch of a dune

The friction factor is assumed to be constant near the dune top. This means that the local dimensionless shear stress θ is proportional to the velocity squared:

$$\theta = \theta_{top}\frac{q^2}{(Y-z)^2}\frac{(Y-H)^2}{q^2} = \theta_{top}\frac{(1-H/Y)^2}{(1-z/H)^2} \tag{12.12}$$

where:

Y = the water depth (m),
H = the dune height (m),
q = the discharge per unit width (m^2/s).

In the case of small transport rates, i.e. bed load only, the local sediment transport can be expressed as a function of θ:

$$\Phi_b = \Phi_b(\theta) \tag{12.13}$$

The spatial variation of Φ_b near the top of the dune is expressed by:

$$\left.\frac{\partial \Phi_b}{\partial x}\right|_{top} = \left.\frac{\partial \Phi_b}{\partial \theta}\right|_{\theta=\theta_{top}} \frac{\partial \theta}{\partial x} = \left.\frac{\partial \Phi_b}{\partial \theta}\right|_{top} \theta_{top} \frac{2}{1 - H/Y} \left.\frac{\partial (z/Y)}{\partial x}\right|_{top} \tag{12.14}$$

where z is the local height of the dune (m).

The migration velocity of the dune c is calculated under the assumption that all of the bed load transport is deposited on the lee side of the dune:

$$c = \frac{q_b}{(1-\varepsilon)H} \tag{12.15}$$

where $q_b = \Phi_b \sqrt{(s-1)gd^3}$ and ε is the porosity of the bed material.

The change in the bed level near the dune top (on the upstream side) can be expressed as:

$$\frac{\partial z}{\partial t} = -c\frac{\partial z}{\partial x} = -\frac{q_b}{(1-\varepsilon)H}\frac{\partial z}{\partial x} \tag{12.16}$$

by use of the continuity equation for sediment:

$$\frac{\partial z}{\partial t} = -\frac{1}{1-\varepsilon}\frac{\partial q_t}{\partial x} \tag{12.17}$$

Equation (12.14) and Equation (12.16) can be related to each other as it follows:

$$\left.\frac{\partial \Phi_b}{\partial \theta}\right|_{top} \left.\frac{2\theta_t}{1 - H/Y} \frac{\partial (z/Y)}{\partial x}\right|_{top} = \left.\frac{\Phi_b}{H/Y} \frac{\partial (z/Y)}{\partial x}\right|_{top} \tag{12.18}$$

or:

$$\frac{H/Y}{1-H/(2Y)} = \left.\frac{\Phi_b}{2\theta\frac{\partial\Phi_b}{\partial\theta}}\right|_{top} \tag{12.19}$$

Equation (12.19) expresses the equilibrium height of the dunes in the case of pure bed load. At the dune top $\partial z/\partial x = 0$ in which case Equation (12.19) does not apply. However, the equation must still hold a short distance upstream of the top where the local dune height is nearly equal to H.

The Dune Height From the Meyer-Peter Bed Load Formula

Fredsøe (1982) used the Meyer-Peter bed load transport rate to give an estimation of the dune height. The Meyer-Peter bed load equation yields:

$$\Phi_b = 8(\theta' - \theta_c)^{3/2} \tag{12.20}$$

Using the Meyer-Peter formulation and Equation (12.19) an expression for the equilibrium dune height can be given as:

$$H = \frac{2Y(\theta' - \theta_c)}{7\theta' - \theta_c} \tag{12.21}$$

Influence of Suspended Load

If the sediment transport consists of both bed load and suspended load the equations are modified as follows:

- The total sediment transport ($\Phi_t = \Phi_b + \Phi_s$) is still assumed to be a function of the local bed shear stress: $\Phi_t = \Phi_t(\theta')$
- Φ_b is replaced by Φ_t in Equation (12.19).
- q_b is retained in Equations (12.14) and (12.16) as it is assumed that only the bed load is deposited at the lee side of the dune.

The general equation describing the equilibrium dune height thus reads:

$$\frac{H/Y}{1-H/(2Y)} = \left.\frac{\Phi_b}{2\theta\frac{\partial(\Phi_b+\Phi_s)}{\partial\theta}}\right|_{top} \tag{12.22}$$

The variation of H/Y as a function of θ is shown in Figure 12.2 for sand with a mean diameter of 0.3 mm using the Engelund & Fredsøe transport model.

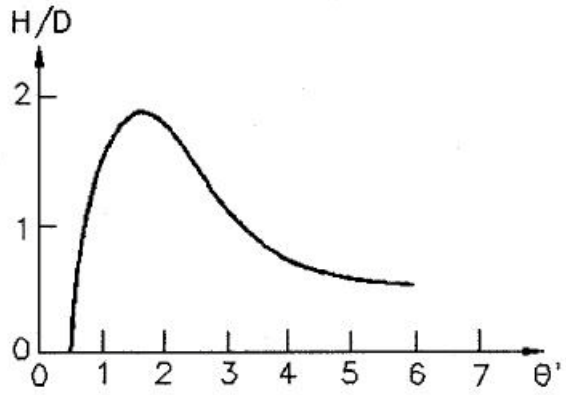

Figure 12.2 *H/Y* as a function of θ'. d_{50} = 0.3 mm

12.2.2 The Equilibrium Dune Length

Fredsøe (1982) has obtained an expression for the equilibrium dune length through a consideration of the dune shape. The end of the dune is defined as the point where $\partial z/\partial x$ is equal to zero, where z is the local dune height. Negative values of $\partial z/\partial x$ will result in diverging flow and, consequently, in very small transport rates. The transported sediment avalanches down the lee slope due to gravity so that the lee slope is very steep.

The dune shape is calculated by use of the continuity equation for sediment in the following way:

a) It has been shown (Engelund & Hansen, 1967) that for bed forms which are travelling downstream with a constant form and celerity c, the height is proportional to the total bed material sediment transport q_t:

$$q_t = (1-\varepsilon)cH + const \tag{12.23}$$

where:

H = dune height,
e = porosity.

If only bed load q_b, is considered, the transport is zero in the troughs and the constant is, therefore, also zero. Thus:

$$q_b = (1-\varepsilon)cH \tag{12.24}$$

b) Fredsøe (1982) found that the length and the form of a dune can be calculated when the dune height, the water depth and the maximum bed shear stress are known.

Fredsøe measured the bed shear stress behind a rearward facing step. He suggested a variation in the local dimensionless bed shear stress θ^* past a dune as:

$$\frac{\theta^*}{\theta^*_{top}} = \frac{\left(1-\frac{H}{2Y}\right)^2}{\left(1+\frac{H}{2Y}-\frac{h}{Y}\right)^2} f\left(\frac{x}{H}\right) \tag{12.25}$$

The function *f(x/H)* is shown in Figure 12.3.

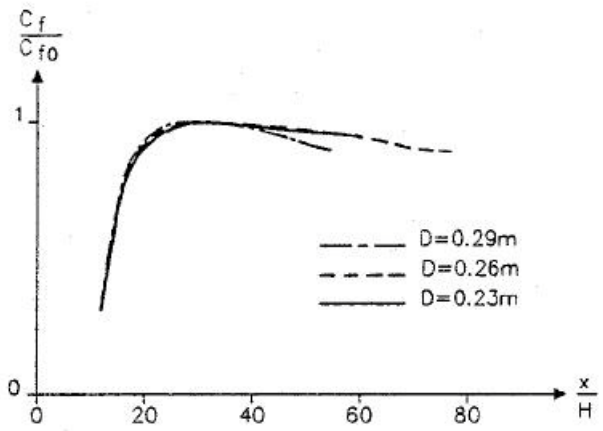

Figure 12.3 Measurements of bed shear stress downstream rearward facing step at different water depths

An expression to *f(x/H)* has been given by Fredsøe:

$$f(x/H) = 3.04\left[0.37 \cdot e^{-\sqrt{\frac{\frac{x}{H}+0.82}{0.82}}}\right] - 0.0045 \cdot \frac{x}{H} \tag{12.26}$$

An alternative expression of *f(x/H)* has been approximated by Rolf Deigaard:

$$f(x/H) = \left(1-e^{-1.059\left(\frac{x}{H}-5\right)}\right) - \left(1.059 - 1/350 \cdot \frac{x}{H}\right) \tag{12.27}$$

The function *f* was assumed to be general, regardless of the shape and size of the dune. The bed load transport along the dune was calculated by use of

the Meyer-Peter bed load formula. The effect of gravity on the bed load q_b, was taken into account by adding to θ the correction:

$$-\mu\frac{\partial z}{\partial x} \qquad giving \qquad q = \sqrt{(s-1)gd^3}\Phi_b\left(\theta - \mu\frac{\partial z}{\partial x}\right) \tag{12.28}$$

where Φ_b is the dimensionless bed load transport, and

$$\mu = \frac{\theta_c}{Tan(27°)} \tag{12.29}$$

For θ_c = 0.05 , μ is approx. = 0.1 .

By combining Equations (12.19) and (12.25) a first order differential equation describing $\partial z/\partial x$ is found:

$$\frac{\partial h}{\partial x} + \left(\frac{\theta^*_{top} - \theta_c}{\mu}\right)\left(\frac{h}{H}\right)^{2/3} = \frac{\theta^* - \theta_c}{\mu} \tag{12.30}$$

The boundary conditions for the problem are:

1. Upstream, where no sediment transport takes place, h is equal to zero at $\theta = \theta^*$
2. θ_{top} is equal to θ^* at the dune top where the dune becomes horizontal.

The value of θ_{max} is not known at the beginning of the integration. A first guess can be $\theta_{max} = \theta_{top}$. An iteration must be carried out in order to achieve the condition: $\theta^* = \theta_{top}$ at the dune top. Which at the same time gives:

$$\left.\begin{array}{l}\dfrac{\partial z}{\partial x} = 0 \\ z = H\end{array}\right\} \qquad for \qquad x = L \tag{12.31}$$

If the dune height (h/H) after the integration is less than 1 when dh/dx becomes negative, then the $qmax$ must be increased. If the dune height is greater than 1, then the value of $qmax$ must be decreased. The iteration is finished when h/H = 1 for dh/dx = 0.

The function f, has a maximum at x = 17 H so this is the length of the dune if the effect of gravity and suspended load is neglected. For small θ_{top} values, however, the effect of gravity is important and causes the dune length to be larger than 17 H.

As indicated above, the calculations are rather laborious and, therefore, the following approximation is suggested for the ratio between the dune height and length for bed load transport only:

$$\frac{H}{L} = \begin{cases} 0.06 - 146(0.15+\theta_c - \theta)^{4.26} & for \quad \theta < 0.15 + \theta_c \\ 0.06 \quad for \quad 0.15 + \theta_c < \theta \end{cases} \tag{12.32}$$

Influence of Suspended Load

The sediment transport has its maximum at the dune crest, see Equation (12.26). The bed load is a function of the local bed shear stress so that the dune crest is the position with maximum bed shear stress for the case of bed load only.

The suspended load is not a function of the local bed shear stress. A spatial lag δ, exists between the hydraulic parameters and the suspended load because it takes some time for the suspended particles to settle or to be picked up from the bed. The spatial lag is given by:

$$\delta = \frac{\varepsilon U_b}{w^2} \tag{12.33}$$

where U_b is the 'slip velocity' and it is defined as:

$$U_b = U_f\left(2 + 2.5\ln\left(\frac{h}{k_s}\right)\right) \approx 15 U_f \tag{12.34}$$

where:

ε	=	the average eddy viscosity: $\varepsilon = 0.077 \cdot U_f \cdot Y$,
U	=	current velocity,
U_f	=	friction velocity,
Y	=	the water depth,
k_s	=	the equivalent sand roughness.

Consequently, the point of maximum transport is moved downstream from the point of maximum bed shear stress. The lag distance is determined from the ratio between the bed load and the suspended load trans-port so that the dune length is given by:

$$L = L_0 + \delta\frac{\Phi_s}{\Phi_s + \Phi_b} \tag{12.35}$$

where L_0 is the dune length for the case of bed load transport only, determined by Equation (12.34).

The dune length as a function of θ' is depicted in Figure 12.4 for 0.3 mm sand.

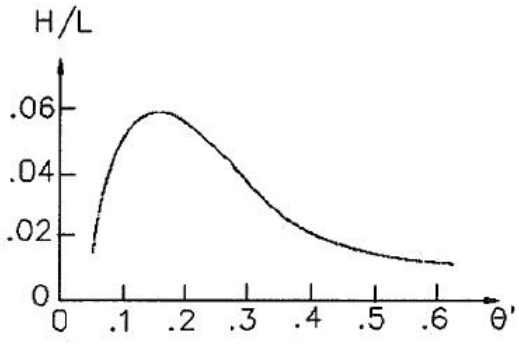

Figure 12.4 The ratio of the dune height and the dune lenght as a function of θ'. d_{50}=0.3mm

12.2.3 Non-Equilibrium Dunes

If the actual dune dimensions deviate from the equilibrium dimensions there is a natural tendency for them to return to the equilibrium condition. This process takes a finite time so a time lag is introduced between the flow conditions and the hydraulic resistance resulting in a hysteretic effect, i.e. the stage-discharge relationship for a water coarse as the discharge increases differs from that as discharge falls.

Non-Equilibrium Dune Height

The rate of change of the dune height has been analysed by Fredsøe (1979). It can be described by the equations used to calculate the equilibrium dune height.

The rate of change of the bed level z, near the dune top is expressed as:

$$\frac{\partial z}{\partial t} = -c \cdot \frac{\partial z}{\partial x} + \frac{dz}{dt} \tag{12.36}$$

where the celerity of the dune front is

$$c = \frac{q_{bt}}{(1-\varepsilon)H} \tag{12.37}$$

where q_{bt} is the transport rate at the dune top, ε is the sediment porosity and $\partial z/\partial t$ is found from the equation of continuity:

$$\frac{\partial z}{\partial t} = \frac{-1}{1-p}\frac{\partial (q_b+q_s)}{\partial x}\bigg|_{top} = \frac{-1}{1-\varepsilon}\frac{\partial (q_b+q_s)}{\partial \theta}\bigg|_{top} - \left(\frac{2\theta_{top}}{1-H/Y}\cdot\frac{\partial z}{\partial x}\cdot\frac{1}{Y}\right) \qquad (12.38)$$

Equations (12.36), (12.37) and (12.38) yield:

$$\frac{dH}{dt} = \frac{1}{1-\varepsilon}\frac{\partial z}{\partial x}\frac{\Phi_b}{H} - \frac{\partial (\Phi_b+\Phi_s)}{\partial \theta}\bigg|_{top} - \frac{2\theta_{top}}{Y-H}\sqrt{(s-1)gd^3} \qquad (12.39)$$

In order to obtain a value of the change of the dune height representative for most of the dunes, the 'integrated' value for $\partial h/\partial x$: H/L is used in Equation (12.41) leading to:

$$\frac{dH}{dt} = \frac{\sqrt{(s-1)gd^3}}{1-n}\frac{1}{L}\bigg|_{top}\Phi_b - \frac{2\theta_{top}}{H/Y-1}\frac{\partial (\Phi_b+\Phi_s)}{\partial \theta}\bigg|_{top} \qquad (12.40)$$

Non-Equilibrium Dune Length

At present no satisfactory theory for the change of dune length exists. The dune length is of less importance for the hydraulic resistance than the dune height, so an approximate description will be sufficient.

A possible definition of the dune length is the total length of a reach divided by the number of dunes within that reach. By this definition, the dune length can (under uniform conditions) only be changed if dunes disappear or new ones are created. Consequently, it seems reasonable to include the average lifetime of a dune in the expression for dL/dt. A plausible assumption is that the average lifetime, T_1, of the dunes can also be used as the time scale for the change in dune length:

$$\frac{dL}{dt} = \frac{L-L_e}{T_1} \qquad (12.41)$$

where L_e is the equilibrium dune length.

A stability analysis shows, if the position of the dune front of a single dune in a row of regular dunes in equilibrium is perturbed, the celerity of the dune c will be reduced regardless of whether the dune front has been advanced or retarded. This implies the dunes are unstable. If the dune front is retarded, the dune will be overtaken by the following dune.

The time required for this process has been estimated from the calculated celerity of the dune when the length has been reduced to $L_e/2$. This celerity is

about 85-90% of the celerity of the equilibrium dunes. It has, therefore, been estimated that the dune will move a distance of the order of magnitude 10 L_e before it is overtaken. T_1 is thus approximately 10 L_e/c, yielding:

$$\frac{dL}{dt} = \left(\frac{L - L_e}{10L_e}\right) \cdot C = \left(\frac{L}{L_e} - 1\right) q_b \cdot \frac{1}{10(1-\varepsilon)H} \tag{12.42}$$

where ε is the sediment porosity.

13 The van Rijn Sediment Transport Model

In the van Rijn sediment transport model (van Rijn, 1984a and 1984b) the sediment transport is divided into bed load and suspended load. The bed load is calculated from the saltation height, the particle velocity and the bed load concentration. The bed load computations follow the approach of Bagnold (1973), which assumes that the motion of the bed load particles is dominated by the gravity forces. When the bed shear velocity exceeds the fall velocity sediment is transported in suspension. The suspended load is calculated as the depth integration of the local concentration and flow velocity. The method uses the reference concentration computed from the bed load transport. The model has been verified for particles in the range 200 - 2000µm. The verification based on 600 data sets, showed that 77% of the predicted bed load rates were within 0.5 and 2 times the observed values, van Rijn (1984a). The verification for the suspended load, using 800 data sets showed that 76% of the predicted values were within 0.5 and 2 times the observed values, van Rijn (1984b).

13.1 The Initiation of Motion

The individual grains lying on the bed are assumed to move when the effective bed shear velocity exceeds the critical bed shear velocity, according to Shields (1936) relationship. Hence,

$$u'_f > u'_{fcr} \tag{13.1}$$

where the critical bed shear velocity is given by:

$$u'_{fcr} = \sqrt{\theta_c (s-1) g d} \tag{13.2}$$

and the effective bed shear velocity u'_f is defined below. u'_f is defined in order to eliminate the resistance from bed forms since the resistance from the form drag does not contribute to bed load transport.

$$u'_f = \frac{u\sqrt{g}}{C'} \tag{13.3}$$

where C' is the Chézy coefficient related to grain roughness given by:

$$C' = 5.75\sqrt{g}\ \log\left(\frac{12R_b}{k_s}\right) \tag{13.4}$$

and R_b is the hydraulic radius related to the bed.

van Rijn assumed the grain roughness height k_s of a plane movable bed to be $3 \cdot D_{90}$, which changes Equation (13.4) to

$$C' = 5.75\sqrt{g}\ \log\left(\frac{4R_b}{D_{90}}\right) \tag{13.5}$$

The critical bed shear stress θ_c is obtained from an analytical function of D_* given by:

$$D_* = d_{50}\left[\frac{(s-1)}{\upsilon^2}g\right]^{1/3} \tag{13.6}$$

For further information on the analytical expression for the critical bed shear stress see the section 7.4 The Critical Bed Shear Stress *(p. 30)*. Note: D_* is similar to D_{gr} defined by Ackers and White in Equation (10.3).

13.2 Bed Load Transport

The bed load is considered to be transported by rolling, sliding and saltation. In the model the bed load transport q_b is computed from the product of particle velocity u_{bs}, the saltation height δ_b and the bed load concentration c_b. Expressions for the particle velocity and saltation height were obtained by numerical solution of the equations of motion for a solitary particle. The bed load is calculated as follows:

$$q_b = u_{bs} \cdot \delta_b \cdot c_b \tag{13.7}$$

where c_b and δ_b are given as functions of the dimensionless particle diameter D_* and the dimensionless transport stage parameter T defined by:

$$T = \frac{(u'_f)^2 - (u'_{fcr})^2}{(u'_{fcr})^2} \tag{13.8}$$

By the use of measured bed load transport rates an expression for the bed load concentration c_b was obtained:

$$c_b = q_b / u_{bs} \cdot \delta_b \tag{13.9}$$

Extensive analysis of the flume measurements for bed load transport, van Rijn (1981), has shown that the bed load concentration can be represented by:

$$\frac{c_b}{c_0} = 0.18\frac{T}{D_*} \tag{13.10}$$

in which c_0 = 0.65, is the maximum bed concentration.

The saltation height δ_b was established by plotting the saltation height as a function of the parameters D_* and T. For the flume experiments it was found that the saltation height could be approximated within 10% by the expression:

$$\frac{\delta_b}{Y} = 0.3D_*^{0.7}T^{0.5} \tag{13.11}$$

The particle velocity was found by use of the general relation derived by Bagnold (1973):

$$\frac{u_b}{u_f} = \alpha_1 + \alpha_2\sqrt{\frac{\theta_c}{\theta}} \tag{13.12}$$

By using the equations of motion for a single particle and the measurements on gravel carried out by Fernandez Luque (1974, 1976) and Francis (1973) the particle velocity was approximated within an inaccuracy of 10% by the expression:

$$\frac{u_b}{u'_f} = 9 + 2.6\log D_* - 8\sqrt{\frac{\theta_c}{\theta}} \tag{13.13}$$

Equation (13.13) was approximated with 20% accuracy by the simpler approximation:

$$\frac{u_b}{\sqrt{(s-1)gd}} = 1.5T^{0.6} \tag{13.14}$$

Combining the above Equations gives the following expression for bed load transport:

$$\frac{q_b}{\sqrt{(s-1)gd_{50}^3}} = \frac{0.053T^{2.1}}{D_*^{0.3}} \tag{13.15}$$

or in a dimensionless form:

$$\Phi_b = \frac{0.053\,T^{2.1}}{D_*^{0.3}} \tag{13.16}$$

13.3 Suspended Load Transport

According to Bagnold (1966), the mode of the sediment transport is assumed to be suspended load when the bed shear velocity exceeds the fall velocity. The calculation of the suspended load is based on the computation of a reference concentration determined from the bed load transport. The reference concentration c_a, is a function of the dimensionless particle diameter D_*, and the transport stage parameter, T:

$$D_* = d_{50}\left[\frac{(s-1)g}{\nu^2}\right]^{1/3} \tag{13.17}$$

where u_f' is the bed shear velocity related to the grains and $u'_{f,cr}$ is the critical bed shear velocity.

The mode of transport of a particle is defined as suspended when the particle is moved a distance of 100 times the particle diameter. The criterion for the initiation of suspension was determined from experimental results (Delft 1982) to be:

$$\frac{u_{*,cr}}{w_s} = \frac{4}{D_*'} \qquad for \qquad 1 < D_* \le 10 \tag{13.18}$$

and

$$\frac{u_{*,cr}}{w_s} = 0.4 \qquad for \qquad D_* > 10 \tag{13.19}$$

van Rijn defines the level of reference the concentration, a, as the level below which all sediment is considered to be transported as bed load. When the height of the bed forms is known the reference level is approximated by:

$$a = 1/2H \tag{13.20}$$

where H is the bed form height.

If the bed form height is not known then van Rijn suggests that the level of the reference concentration can be taken as the roughness height, k_s:

$$a = k_s \tag{13.21}$$

with a minimum value of:

$$a = 0.01\,Y \tag{13.22}$$

where Y is the water depth (m).

The reference concentration is defined from:

$$q_b = c_b u_{bs} \delta_b = c_a u_a a \tag{13.23}$$

where:

c_b	=	the bed concentration,
u_{bs}	=	the velocity of bed load particles,
δ_b	=	the saltation height.

The expressions for these parameters are given under 13.2 Bed Load Transport *(p. 68)*. This assumes that the effective particle velocity, u_a at reference level a can be given as:

$$u_a = \alpha u_{bs} \tag{13.24}$$

By use of the proposed relation for the bed load concentration c_a can be expressed as:

$$c_a = \frac{0.035}{\alpha_2} \frac{d}{a} \frac{T^{1.5}}{D_*^{0.3}} \tag{13.25}$$

From an examination of flume and field data a value for α of 2.3 was determined, giving:

$$c_a = 0.015 \frac{d_{50}}{a} \frac{T^{1.5}}{D_*^{0.3}} \tag{13.26}$$

The representative particle size of suspended load is generally finer than the size of the bed load particles. van Rijn relates this particle size d_s to the d_{50} and the geometric standard deviation σ_s of the bed material:

$$\frac{d_s}{d_{50}} = 1 + 0.011\,(\sigma_s - 1)(T - 25) \qquad for \qquad T \le 25$$
$$d_s = d \qquad for \qquad T > 25 \tag{13.27}$$

in which σ_s is given by:

$$\sigma_s = 0.5\left(\frac{d_{84}}{d_{50}} + \frac{d_{16}}{d_{50}}\right) \tag{13.28}$$

The d_s value is then used to calculate fall velocity according to the Equations (7.8), (7.9) and (10.3). The description of the suspended load is based on the solution of the integral:

$$q_s = \int_a^Y cu\,dy \tag{13.29}$$

van Rijn solves the integral as:

$$q_s = \frac{u_f c_a}{\kappa}\left[\frac{a}{Y-a}\right]^{Z'}\left[\int_a^{0.5Y}\left[\frac{Y-y}{y}\right]^{Z'} Ln\left(\frac{y}{y_0}\right) + \int_{0.5Y}^{Y}\exp\left(-4Z'\left(\frac{Z}{Y}-0.5\right)Ln\left(\frac{y}{y_0}\right)\right)dy\right] \tag{13.30}$$

In the expression above, Z expresses the influence of the upward turbulent fluid forces and the downward gravitational forces. Z is defined as:

$$Z = \frac{w}{\beta\kappa u'_f} \tag{13.31}$$

where:

u_f'	=	the overall bed shear velocity,
κ	=	von Karman's constant,
β	=	a coefficient related to the diffusion of sediment particles.

An expression for β was derived as:

$$\beta = 1 + 2\left[\frac{q}{ubf}\right]^2 \qquad for \qquad 0.1 < \frac{w}{u'_f} < l \tag{13.32}$$

Z' is the modified suspension number given as:

$$Z' = Z + \psi \tag{13.33}$$

where the overall correction factor ψ represents all additional effects (volume occupied by particles, reduction of fall velocity and damping of turbulence). ψ was found to be a function of the main hydraulic parameters:

$$\psi = 2.5\left[\frac{w}{u'_f}\right]^{0.8}\left[\frac{c_a}{c_o}\right]^{0.4} \qquad for \qquad 0.1\text{-}1 \tag{13.34}$$

where c_0 = 0.65, is the maximum bed concentration.

An approximation to Equation (13.32) was given by van Rijn within an accuracy of 25%:

$$q_s = FuYc_a$$
$$for \qquad 0.3 \le Z' \le 3 \quad and \quad 0.01 \le a/Y \le 0.1 \tag{13.35}$$

F is given by:

$$F = \frac{\left[\frac{a}{D}\right]^{Z'} - \left[\frac{a}{D}\right]^{1.2}}{\left[1 - \frac{a}{D}\right]^{Z'}[1.2 - Z']} \tag{13.36}$$

13.4 Flow Resistance - van Rijn

13.4.1 Bed Forms and Alluvial Roughness

van Rijn (1984) assumes that the bed form dimension are mainly controlled by the bed load transport. The bed load is described as:

$$q_b = u_{bs} \cdot \delta_b \cdot c_b \tag{13.37}$$

where:

q_b = the bed load,
c_b = the bed load concentration,
δ_b = the thickness of the bed layer,
u_b = the velocity of the bed load particles.

By use of kinematic considerations the continuity equation for bed load can also be formulated as:

$$q_b = (1-\varepsilon)\alpha H u_s \tag{13.38}$$

where:

ε = the porosity,
α = shape factor for the dunes,
H = the height of the bed forms,
u_d = the migration velocity of the dunes.

By the use of the functional relationships derived for the bed load transport, van Rijn found that the height and the length of the bed forms can be expressed as:

$$\frac{H}{Y} = f\left(\frac{d}{Y}, D_*, T\right) \tag{13.39}$$

$$\frac{L}{Y} = f\left(\frac{d}{Y}, D_*, T\right) \tag{13.40}$$

where:

H = the height of the bed forms,
L = the length of the bed forms.

van Rijn used a large quantity of field data to decide the functional relationships for the dune height and the dune length. He found no significant influence from D_* on the bed form dimensions, and found the following best fitting equations:

The dune height:

$$\frac{H}{Y} = 0.11 \cdot \left(\frac{d}{Y}\right)^{0.3} \cdot (1 - e^{-0.5T}) \cdot (25 - T) \tag{13.41}$$

The dune length:

$$\frac{H}{L} = 0.015 \cdot \left(\frac{d}{Y}\right)^{0.3} \cdot (1 - e^{-0.5T}) \cdot (25 - T) \tag{13.42}$$

or by inserting equation (13.42) into equation (13.41):

$$\frac{L}{Y} = 7.3 \tag{13.43}$$

The height of the bed forms has a maximum at $T = 5$ and it is assumed that the surface of the bed is almost flat for $T < 0$ or $T > 25$.

13.4.2 Alluvial Resistance From Bed Forms

van Rijn calculates the total alluvial friction as the sum of the skin friction and the form friction:

$$k_b = k' + k'' \tag{13.44}$$

For a flat movable bed, van Rijn relates the effective grain roughness to the skin friction with the expression:

$$k_s = 3D_{90} \tag{13.45}$$

In order to describe the form roughness, van Rijn uses the functional relationship introduced by Yalin (1972):

$$k'' = f(H, H/L) \tag{13.46}$$

From flume and field data van Rijn found the form friction to be:

$$k'' = 1.1H \cdot (1 - e^{-25H/L}) \tag{13.47}$$

The total alluvial friction can then be written as:

$$k = 3D_{90} + 1.1H \cdot (1 - e^{-25H/L}) \tag{13.48}$$

Finally the Chézy coefficient can be computed as:

$$C = 18\log\left(\frac{12R_b}{k_b}\right) \tag{13.49}$$

14 Sediment Transport at Structures

14.1 Sediment Transport in Manholes

The sediment transport in manholes is routed straight through the manhole without any deposition. This is done as the level of turbulence is high in manholes and hence it is assumed that the sediment is transported in suspension. Further, insufficient field data is available to predict deposition, if any, in manholes. The sediment transport from a manhole is distributed according to the ratio of the outflowing discharges. A userdefined disribu-tion can also be specified by giving the coefficients and exponents (*K* and *n* values) in the following relationship:

$$S_{t3}^{n+1} = \frac{K_3 \cdot Q_3^{n3}}{K_3 Q_3^{n3} + K_4 Q_4^{n4}} (S_{t1}^{n+1} + S_{t2}^{n+1}) \tag{14.1}$$

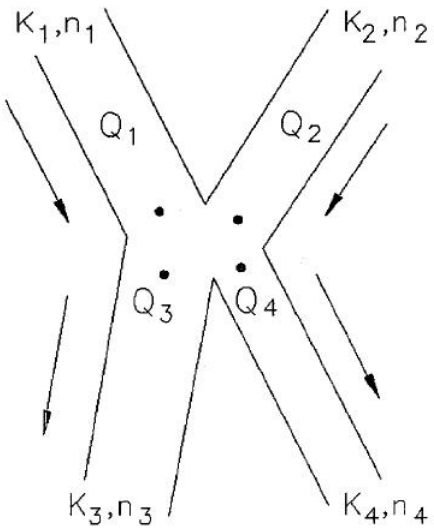

Figure 14.1 Distribution of sediment according to discharge

14.2 Sediment Transport in Basins

Sediment can be removed from basins according to the formula:

$$E = 1 - \left(1 + \frac{1}{n} \frac{w}{Q/A}\right)^{-n} \tag{14.2}$$

where:

E	=	the sediment trap efficiency,
w	=	the fall velocity,
q	=	the discharge into the tank,
a	=	the surface area of the basin,
n	=	turbulence constant indication the settling performance of the basin:

n = 1, for poor performance,
n = 3, for good performance,
n > 5, very good performance,
n = ∞, ideal performance.

The sediments removed by the Equation (14.2) are taken out of the computations. Hence, no morphological modelling takes place of the deposited sediment and it is not possible to re-suspend this sediment.

14.3 Sediment Transport in Overflow Structures

The sediment transport over a weir can be modelled in three different ways:

a) $S_{weir} = (1 - reduction_{factor}) \cdot S_{Total\ into\ weir}$

b) $S_{weir} = (1 - Eff(Q)) \cdot S_{Total\ into\ weir}$

c) $S_{weir} = (1 - Eff(w/v_0)) \cdot S_{Total\ into\ weir}$

ad a)the reduction factor is constant throughout the whole simulation,

ad b) the reduction factor is a function of the discharge flowing into the weir,

ad c) the reduction factor is given as the expression below:

$$Eff\left(\frac{w}{v_0}\right) = 1 - K \cdot \mathrm{Exp}\left(-\left(\frac{w/v_0 - \mu}{\sqrt{2} \cdot \sigma}\right)^2\right) \quad (14.3)$$

Where K, μ and σ are dimensionless variables given as:

$$\begin{aligned} K &= k_1 \cdot Q_{out}/Q_{in} + k_2 \\ \mu &= \mu_1 \cdot Q_{in}/(Q_{in} - Q_{out}) + \mu_2 \\ \sigma &= \sigma_1 \cdot Q_{in}/(Q_{in} - Q_{out}) + \sigma_2 \end{aligned} \quad (14.4)$$

Where k_1, k_2, μ_1, μ_2, σ_1 and σ_2 are user defined constants.

Equation (14.3) has been approximated for the central weir and the swirl separator as, Ref. Morten Steen Sørensen, 1991.

The Central Weir:

$$\begin{aligned} K &= -140.697 \cdot Q_{out}/Q_{in} + 133.86 \\ \mu &= -2.308 \cdot Q_{in}/(Q_{in} - Q_{out}) + 3.17 \\ \sigma &= 1.617 \cdot Q_{in}/(Q_{in} - Q_{out}) - 0.27 \end{aligned} \quad (14.5)$$

The Swirl Separator:

$$\begin{aligned} K &= -79.782 \cdot Q_{out}/Q_{in} + 133.54 \\ \mu &= -5.015 \cdot Q_{in}/(Q_{in} - Q_{out}) + 3.92 \\ \sigma &= 2.659 \cdot Q_{in}/(Q_{in} - Q_{out}) - 0.22 \end{aligned} \quad (14.6)$$

14.4 Sediment Transport in Pumps

The sediment transport in pumps is modelled as an instantaneous transport from the pump node to the destination (tail) node of the pump. This simplification is done as insufficient data is available in MOUSE to model the transport in the rising mains. It is important to keep this constraint in mind when simulating sediment transport in pumped systems.

15 Modelling of Adhesive Sediments

In sewers, adhesive forces may exist between the particles in the sediment deposits. The critical bed shear stress has been found to be much larger for particles with adhesive properties than the Shields criterion. It has been shown that when the critical bed shear stress has been exceeded for the sediment with the adhesive properties they are transported as non-cohesive sediment particles.

The adhesive forces are dependent on various different parameters such as: the time since the deposition, the chemical and biological process in the sewer and the sediment characteristics. Insufficient data exist to give a description of the development of the adhesive forces between the sediment particles. Hence, the development of adhesion between the sediment particles is not modelled in MOUSE ST, but it is possible to give variation of the critical bed shear stress in the initial sediment deposits in the sewer system. As long as only erosion occurs, the critical bed shear stress is calculated according to the function given for the critical bed shear stress given for the adhesive sediments. If deposition occurs, the critical bed shear stress is set equal to the Shields critical bed shear stress, and Shields critical bed shear stress will be used as long as the depth of the sediment deposit is larger than the maximum depth to which the initial sediment deposit has been eroded. The formulation of the critical bed shear stress is given below.

If the actual sediment depth is larger than the maximum eroded sediment depth, then

$$\theta_c = \theta_{c,\,Shields}$$

$$else$$

$$\theta_c = \theta_{bot} + (\theta_{top} - \theta_{bot}) \cdot \left(\frac{y_{sediment}}{y_{initial\ depth}} \right)^{FAC} \tag{15.1}$$

where:

θ_{bot}	=	the critical bed shear stress at the bottom of the pipe,
θ_{top}	=	the critical bed shear stress at top of the initial sediment deposit,
$y_{sediment}$	=	the actual depth of the sediment deposit,
$y_{initial\ depth}$	=	the initial depth of the sediment deposit.

16 Sediment Transport in Pipes With a Thin Layer of Sediment

If the sediment depth in a pipe is less that the equilibrium dune height for the corresponding flow conditions the morphological sediment transport is modified in the following way:

$$Fix_{bed} = \frac{Z_{dune}}{Z_{sediment}} \tag{16.1}$$

$$\begin{aligned} &If\ \ Fix_{bed} < 0.5 \quad then \\ &Sed_{reduction\ factor} = 2 \cdot Fix^2{}_{bed} \\ &else \\ &Sed_{reduction\ factor} = 1 - (1 - Fix_{bed})^2 \end{aligned} \tag{16.2}$$

$$S = S_{reduction\ factor} \cdot S_{full\ transport\ capacity} \tag{16.3}$$

The Equations (16.1) - (16.3) describe the reduction in the sediment transport due to the fact that the sediment depth in the pipe is less than the bed load transport layer (the equilibrium dune height). The reduction factor is shown as a function of the sediment depth over the equilibrium dune height in Figure 16.1.

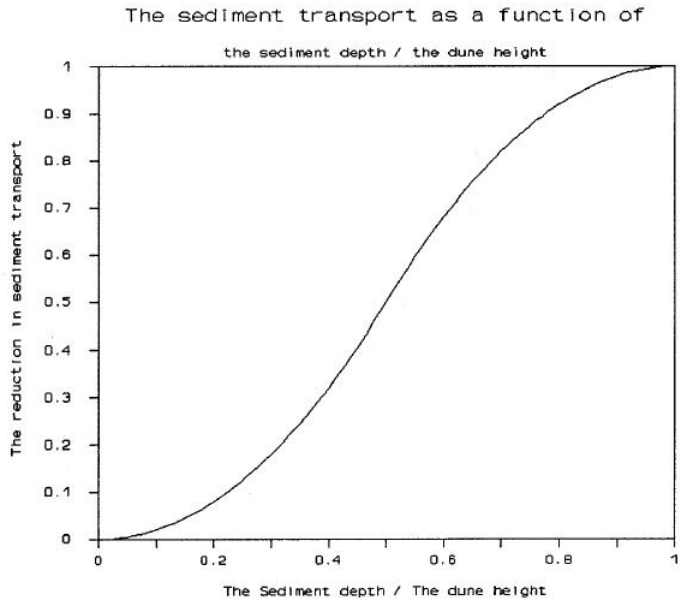

Figure 16.1 The reduction in sediment transport as a function of the sediment depth over the dune height

17 The Morphological Model

17.1 Numerical Solution

The morphological model is the numerical solution of the continuity equation for sediment transport. The continuity equation for sediment yields:

$$W\frac{\partial S}{\partial x} + (1-\varepsilon)\cdot\frac{\partial Z}{\partial t} = 0 \tag{17.1}$$

The sediment continuity equation is solved by use of a Preissmann Scheme, see Figure 17.1.

$$\begin{aligned}&1-\varepsilon)\left[(1-\psi)\frac{W\Delta z_j^{n+1}}{\Delta t} + \psi\frac{W\Delta z_{j+1}^{n+1}}{\Delta t}\right] \\ &\vdash \theta\frac{S_{j+1}^{n+1} - S_j^{n+1}}{\Delta x} + (1-\theta)\frac{S_{j+1}^{n} - S_j^{n}}{\Delta x} = 0\end{aligned} \tag{17.2}$$

Where:

W	=	the flow width (m),
Δz^{n+1}	=	the change in bed level (m),
s^n_j	=	the sediment transport rate per unit width (m^2/s),
S^n_j	=	$W \cdot s^n_j$,
ε	=	the porosity of the sediment,
ψ	=	the space centring coefficient ($0.5 \le \psi \le 1$),
θ	=	the time centring coefficient ($0.5 \le \theta \le 1$).

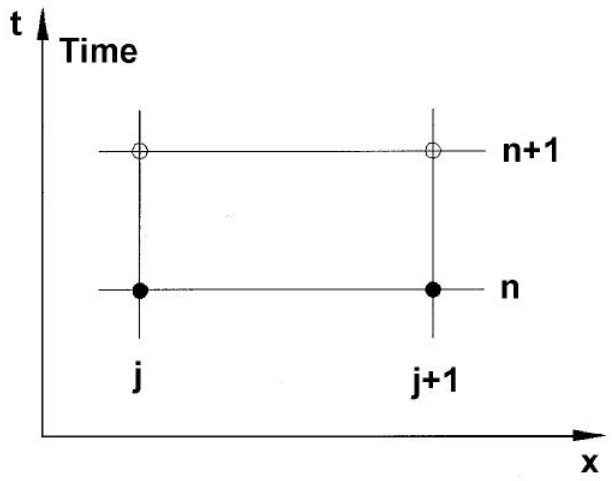

Figure 17.1 The Preissmann scheme

The transport at $t = (n+1)\Delta t$ is approximated by:

$$S_j^{n+j} = s_j^n + \left(\frac{\partial s}{\partial U}\frac{\partial U}{\partial z} + \frac{\partial s}{\partial Y}\frac{\partial Y}{\partial z}\right)_j \Delta z_j^{n+1} \tag{17.3}$$

or, introducing the term α:

$$s_j^{n+1} = s_j^n + \alpha \Delta z_j^{n+1} \tag{17.4}$$

$\partial U/\partial z$ and $\partial Y/\partial z$ are by default calculated assuming locally steady flow (back-water curve). In this case, $\partial Y/\partial z$ and $(\partial U/\partial z)\cdot(Y/U)$ will normally be close to -1 and 1, respectively. It is also possible to select:

$$\frac{\partial Y}{\partial z} = -1 \qquad \textit{and} \qquad \frac{\partial U}{\partial z}\frac{Y}{U} = +1 \tag{17.5}$$

what is probably a better approximation in strongly unsteady flow.

$\partial s/\partial U$ and $\partial s/\partial Y$ are obtained by numerical differentiation, e.g.

$$\frac{\partial s}{\partial U} \approx \frac{s(U + \Delta U, Y) - s(U, Y)}{\Delta U} \tag{17.6}$$

or

$$\frac{\partial s}{\partial U} \approx \frac{s(U \cdot fac, Y) - s(U, Y)}{U \cdot fac - U} \tag{17.7}$$

where

$$fac = \frac{U + \Delta U}{U} \tag{17.8}$$

17.2 The Boundary Conditions To the Morphological Model

The unknown variable in the finite difference scheme is the bed level, *z*. This becomes evident by substituting Equation (17.2) into Equation (17.1). The boundary conditions should therefore be given in terms of bed level variations. However, a sediment transport boundary condition may be given. In this case the difference between the transport specified at the boundary and the calculated transport at the in-flow point is assumed to erode/deposit at the inflow point, (one point continuity), i.e.

$$S_{BND} / W - (S_j^n + \alpha \Delta z_j^{n+1}) = \frac{\Delta x}{\Delta t}(1 - \varepsilon)\Delta z_j^{n+1} \tag{17.9}$$

Equation (17.2) is solved for Δz_j^{n+1}.

The boundary conditions must be given at all inflow boundaries. Hence, boundary conditions should also be given on a boundary where the water level is varying as a function of time if alternating in- and outflow occur.

The Preissmann scheme is well suited for the solution of hyperbolic problems with only one characteristic. However, it has a drawback. At small Courant numbers it may generate short wave oscillations (wave length $2\Delta x$). The oscillations can be damped by space forward centring the scheme (i.e. by using a large value of ψ). This, however, gives rise to numerical dispersion at high Courant numbers. An option for automatic selection of the optimum value of ψ can be incorporated, i.e. the value which just prevents the short wave oscillations to occur. The factor "*fac*", used in the numerical differentiation of the sediment transport formula, should not be made too small because this will give rise to "overshoot" phenomena in the numerical solution. A value of about 1.5 will be on the safe side in most cases unless very strong gradients occur. The sediment transport Courant number is of the order of magnitude:

$$5 \frac{\Delta t}{\Delta x} \frac{s}{Y} \frac{1}{1 - \varepsilon} \tag{17.10}$$

This implies that the morphological model can run with a much larger time step than the hydrodynamic model. Often the time step will be limited only by the ability to resolve the boundary conditions, together with the disturbance from the updating of the bed level. This disturbance should be sufficiently small in order not to introduce instabilities in the hydrodynamics. A time step

in the order of 6-10 times the time step in the hydrodynamic calcula-tion is suggested.

18 Graded Sediments

Real sewer sediments are often non-uniform and the sediment transport is much more complex than the case of uniform sediments. E.g. smaller particles are sheltered by bigger particles and therefore transported at another rate. Larger particles are exposed to larger fluid dynamic forces compared to uniform sediment and hence they are transported at a larger rate. At low values of the bed shear stress the coarse fraction might not move at all and hence an armouring of the bed might take place. When the bed shear is much lager than the critical bed shear stress the use of a single representative grain size is acceptable.

Non-uniform sediments in which the sediment transport can be calculated by fraction and the variation in time and space of the particle size distribution determined. As an approximate guide the graded sediment module should be used where the bed shear stress is close to the critical value for erosion.

For the simulation of graded sediments and sediment sorting the bed material is considered to comprise two layers: an active layer overlying a passive layer. This is illustrated in Figure 18.1. The active layer is the layer within which most transport occurs. Its depth is intuitively defined as 1/6 of the water depth on a plane bed the dune height. If erosion of the bed material occurs, the composition of the material in the passive layer stays the same. However, if deposition occurs active bed material is (instantaneously) mixed with the material in the passive layer and the composition is modified accordingly.

The additional input data required to simulate the transport of graded sediment are the initial percentage size distributions of both the active and passive layer (they may have the same distribution initially). The data are specified as a number of fractions *N*, and the corresponding percentage and mean grain size of fraction. This percentage varies as sediment is transported selectively and mixed between layers.

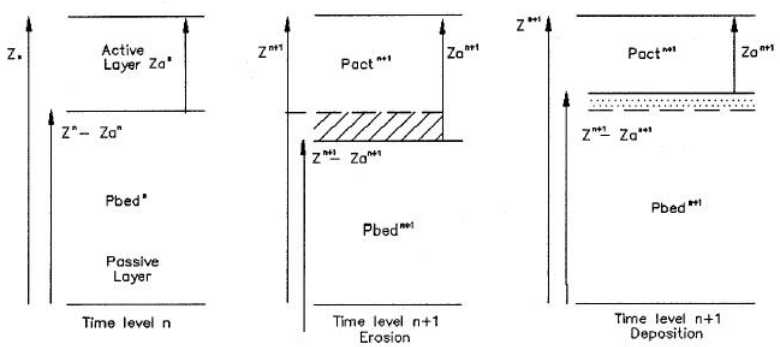

Figure 18.1 The active and the passive layers for the simulation of graded sediments

The transport and mixing of graded sediments is simulated in the following manner. The sediment transport is calculated for each specified class size separately. The calculation is modified in two ways from the calculation of a uniform material. Firstly, the criterion for the threshold of movement (θ_c or A in the Ackers and White Model) is modified to allow for the hiding of finer particles and the greater exposure of larger particles as well as the mutual interference between particles of different size. θ_c is modified by applying Egiazaroff's (1965) correction factor, as follows:

$$\theta_{ci} = \theta_c \left[\frac{\ln(19)}{\ln\left(\frac{19 d_i}{d_{med}}\right)} \right]^2 \tag{18.1}$$

where:

θ_{ci}	=	the dimensionless critical bed shear stress for class i,
θ_c	=	the dimensionless critical bed shear stress for uniform sediment,
d_i	=	the representative grain size in class i,
d_{med}	=	the representative class size of the total sediment population.

For the Ackers and White Model, the modified value of A is expressed as follows (Ackers and White, 1980):

$$A_i = A(d_i / d_{med})^{-0.2} \tag{18.2}$$

where:

A_i	=	the critical flow mobility number for class i,
A	=	the critical flow mobility number for uniform sediment.

The second modification is to multiply each class sediment transport, qt_i by its percentage contribution p_i. After the transport rate in each class has been calculated, the total transport qt is determined by summation over all classes N:

$$qt = \sum_{i=1}^{N} qt_i \cdot p_i \tag{18.3}$$

The sediment continuity equation is then solved in the same way as for uniform sediment, using the total transport to obtain the change in bed level Δz. Once Δz is known, the sediment continuity equation is then solved for each class size, using the class transport rate qt_i and the total bed level change Δz

to obtain the new percentage contribution of the active layer p_i. The sediment continuity equation for each fraction may be expressed as:

$$(1-\varepsilon)\frac{\partial W\overline{p_i Z}}{\partial t}+\frac{\partial qt_i}{\partial x}=0 \tag{18.4}$$

where:

ε	=	sediment porosity.
W	=	channel width.
$\overline{p_i Z}$	=	the average proportion of class *i* in both passive and active layer (i.e. over depth *Z*).

Expanding the first term of Equation (18.4) gives:

$$(1-\varepsilon)\frac{\partial W\overline{p_i Z}}{\partial t} = (1-\varepsilon)\left[\left(\frac{\partial Wp_i Z}{\partial t}\right)_j \psi+\left(\frac{\partial Wp_i Z}{\partial t}\right)_{j-1}(1-\psi)\right] \tag{18.5}$$

in which the time derivative is expressed by:

$$\Psi\left(\frac{\partial Wp_i Z}{\partial t}\right)_j = \frac{W_j}{\Delta t}t[(p_i Z)^{n+1}-(p_i Z)^n]\Psi \tag{18.6}$$

For the time derivative in Equation (18.4) the following expressions apply. For the case of erosion:

$$(p_i Z)_j^{n+1} = [p_{act}^{n+1}\cdot Z_a^{n+1}-\Delta Z^{n+1}p_{bed_i}^{n+1}]_j \tag{18.7}$$

and for deposition:

$$(p_i Z)_j^{n+1} = [p_{act_i}^{n+1}\cdot Z_a^{n+1}+0.5\Delta Z^{n+1}]_j \tag{18.8}$$

In the above expressions, Z and Z_a are as defined in Figure 18.1, and Z_a is the depth of the active layer. p_{acti} and p_{bedi} are the percentage contributions of class *i* in the active and passive layers respectively, and *n+1* refers to the time level at $n+\Delta t$.

Similarly, a weighted time average is used to expand the space derivative in the transport term in Equation (18.4).

$$\frac{\partial q_{ti}}{\partial x} = \frac{q_{ti,j}-q_{ti,j-1}}{\Delta x} = \frac{(1-\theta)(q_{ti,j}-q_{ti,j-1})}{\Delta x}+\frac{\theta(q_{ti,j}^{n+1}-q_{ti,j-1}^{n+1})}{\Delta x} \tag{18.9}$$

where q_{ti}^{n+1} is approximated by:

$$q_{ti}^{n+1} = p_{act_i}^{n+1} \cdot q_t^{n+1} - p_{act_i} \cdot q_t^{n+1} + q_{ti} + \Delta Z^{n+1} \cdot \alpha_i^{n+1} \quad (18.10)$$

$$\alpha_i = \left(\frac{\partial q_{ti}}{\partial u} \cdot \frac{\partial u}{\partial z} + \frac{\partial q_{ti}}{\partial D} \cdot \frac{\partial D}{\partial Z} \right) \quad (18.11)$$

and is calculated for each fraction.

The above expressions, are then solved for the unknowns p_{acti} and p_{bedi} time level *n+1*.

19 Nomenclature

a thickness of the bed layer,

A critical flow mobility number in Ackers and White model,

A hydraulic area,

A_i critical flow mobility number in Ackers and Whitemodel for class *i*,

c concentration of suspended sediment,

c migration velocity of dune,

c_b concentration of suspended sediment at the bed,

C model parameter in Ackers and White Model,

d grain size,

d_i representative grain size in class *i*,

d_{med} representative grain size of total population,

d_n grain diameter for which *n%* of the sample is finer,

D_{gr} dimensionless grain diameter,

D pipe diameter,

D_* particle number,

F Froude number,

F_D drag force (*N*),

F_{gr} general mobility parameter,

g acceleration due to gravity (9.81 m/s2),

G_{gr} general transport parameter,

h local dune height,

H maximum dune height,

I the slope of the energy line,

I_B the bed slope,

k the wave number,

$k_s$equivalent sand roughness,

*L*dune length,

$L_e$equilibrium dune length,

*m*model parameter in Ackers and White model,

*M*the Manning number (*1/n*),

*n*Manning roughness coefficient (*1/M*),

*n*model parameter in Ackers and White model,

*N*number of classes in a graded sediment,

*p*probability for particles to move,

$p_i$percentage contribution in class *i*,

*P*wetted perimeter,

*q*flow discharge per unit width,

$q_b$bed load transport rate,

$q_s$suspended load transport rate,

$q_t$total load transport rate,

q_{ti}total load transport rate in class *i*,

*Q*flow discharge,

*R*hydraulic radius,

R_e Reynolds Number,

*s*relative density of sediment,

s^n_jsediment transport rate per unit of width at grid point *j* and time interval *n*,

$s^n_{j\ si,j}$sediment transport rate per unit of width at grid point *j* and time interval *n* in class *i*,

s_j^nsediment transport rate at grid point *j* and time interval *j* (= W_{sjn}),

*t*sediment bed thickness,

*T*parameter dependent on *u, Y, d* (see equation (10.14) under flow Resistance - White et al.),

u mean flow velocity,

u_b velocity of bed load particles,

u_f friction velocity,

w fall velocity,

w_e effective bed width,

W width of the flow,

x coordinate in flow direction,

X sediment transport, mass flux per unit mass flow rate,

y distance above bed level,

y' thickness of the boundary layer,

Y water depth,

z the bed level,

z local height of a dune,

Z the Rouse number,

Δz change in bottom level,

Z_a depth of active layer,

α velocity distribution coefficient,

β dynamic friction coefficient,

δ spatial lag,

ε porosity of sediment,

E eddy viscosity,

λ_b linear concentration related to c_b,

C space centring coefficient,

ρ fluid density,

θ time centring coefficient,

θ dimensionless bed shear stress,

θ_c critical dimensionless bed shear stress,

θ_{ci}critical dimensionless bed shear stress for class *i*,

θ'dimensionless skin friction,

θ''dimensionless form friction,

θ_{max}maximum dimensionless shear stress at the dune,

θ_{top}dimensionless shear stress at the dune top,

θ_*local dimensionless shear stress,

μconstant defined in Equation (12.29),

*v*kinematic viscosity,

τbed shear stress,

$\tau_c$critical bed shear stress,

τ'skin friction,

τ''form drag,

Φdimensionless sediment transport rate,

$\Phi_b$dimensionless bed load sediment transport rate,

$\Phi_s$dimensionless suspended sediment load transport rate,

$\Phi_t$dimensionless total sediment transport rate.

MOUSE POLLUTION TRANSPORT

Reference Manual - Advection Dispersion

20 Introduction

Driven by ever-increasing legal requirements and public interest, emissions of pollution from urban sewer and drainage systems into the receiving waters become, both in quantitative and qualitative terms, a focus of particular interest in many evaluations of the system's performance. The knowledge of temporal and spatial distribution of water discharges at outlets and at combined sewer overflows (CSOs), generated by hydrodynamic model simulations, provides useful information about the system operation under given conditions. However, this information is insufficient for the evaluation of e.g. dynamics of the pollution loads at the wastewater treatment plant or the real scale of the problem associated with CSOs. In order to fulfil the articulated demand, the simulation tools must include the description of the pollution transport process.

Transport of pollutants in sewer networks is an extremely complex process and cannot be described with a single transport mechanism. This complexity is due to the nature of the transported pollutants. These occur both as dissolved matter and as pollutant particles. The particulate phase of sewage-borne pollution includes a wide range of particle sizes, which implies various transport mechanisms. E.g. extremely fine suspended pollutant particles (so called "wash-load") behave practically as dissolved. On the other hand, pollutants are attached to the sediments of various grain sizes, which can either be transported as suspended or as bed load, depending on the actual grain size and hydraulic conditions.

The variety of pollutants and their forms in sewage include further complication to the understanding of pollution transport in sewers. Certain types of pollutants occur exclusively in dissolved form, while some other appear only as particles. Organic pollution (e.g. expressed as BOD) is present both in dissolved and particulate phase, with the possibility to move between the suspended and bed load.

Hence, a comprehensive description of the pollution transport process, appropriate for practical numerical modelling applications, must essentially be constituted of several fundamentally different formulations. Transport of dissolved pollutants can successfully be described by the Advection-Dispersion (AD) formulation. This formulation, implemented in MOUSE AD, is based on mass continuity and advection-dispersion equations, where phenomena like mass conservation, advective transport, molecular and turbulent diffusion and the diffusive effect from the non-uniform velocity distribution are included.

Experience shows that the AD formulation can also be used for the simulation of suspended (fine) fraction of particulate pollutants and sediments. Hence, MOUSE AD is essential for the simulation of sediment transport processes (suspended sediment fractions), with or without interaction of sediments and pollutants.

Thus, MOUSE AD is a cornerstone of the MOUSE Pollution Transport suite, essential for the analysis of temporal and spatial distribution of pollution emissions, WWTP loading patterns, morphological studies, etc.

The AD module is also the basic foundation of the water age module.

This Technical Reference manual provides an insight into the theoretical aspects of the numerical solution implemented in MOUSE AD. In association with the user guide, this manual should be sufficient for a sensible and effective use of the AD module.

21 Sources of Dissolved Substances in Sewer Systems

Dissolved substances in sewers originate from several sources. These are:

- surface runoff,
- build up in gully pots during dry weather,
- infiltration,
- waste water.

The sources are described in more detail below.

21.1 Dissolved Substances in Surface Runoff

Dissolved substances in surface runoff consist of two components:

- dissolved substances in the precipitation,
- wash-off from the surface.

Precipitation is far from clean. As it passes though the atmosphere, there is an uptake of substances such as nutrients, organic material, solids, metals and pesticides. American researchers have found higher levels of ammonia in precipitation than in runoff from the residential areas and they found that nitrate in the precipitation in some urban areas accounted for 20-90 % of the nitrate in the storm water runoff. The remaining part of the dissolved substances in the surface runoff comes from the erosion of mass on the surface by surface runoff.

21.2 Build up of Dissolved Substances in Gully Pots

The purpose of a gully pot is to trap particles and to prevent them from entering the pipe system. Also, gully pots prevent the release of odour from the pipe system. During dry weather, the amount of dissolved pollutants (e.g. ammonia) builds up in the gully pot liquid. The rate of build up is dependent on the type of pollutant, the biological/chemical conditions in the gully pot and the temperature. During rain storms, the gully pot liquid mixes with the incoming rain water and the polluted water is released. Under some circumstances this phenomena contributes significantly to the First Foul Flush.

21.3 Infiltration Into the Sewer System

Few data are available describing the concentrations in infiltration water. It is often assumed to be clean due to its origin in the soil layers. Infiltration originates from three sources:

- antecedent precipitation,
- frozen residual moisture,

- ground water.

If the quality of the ground water is known or an infiltration study has been carried out, the concentrations of the infiltration can be estimated from these.

21.4 Wastewater

Wastewater originates from residential, commercial and industrial sources. The concentrations of the dissolved substances in the wastewater strongly depend on the local conditions e.g. land use type, number of inhabitants in the catchment and type of industry. Typically, concentrations in wastewater vary on an hourly and daily basis.

22 Transport of Dissolved Substances in Sewer Systems

The transport of dissolved substances is traditionally described by the advection-dispersion equations. These equations describe the one-dimensional mass-conservative transport of dissolved material.

The advection-dispersion equation needs inputs from a hydrodynamic model in terms of water levels and discharges. The hydrodynamic basis of the MOUSE advection-dispersion model is the hydrodynamic model in MOUSE. This model solves the full St. Venant equations for looped systems with free surface flow or pressurized flow. The hydrodynamic model is described in the MOUSE user guide and reference manual.

The main assumptions of the one dimensional advection-dispersion equation are:

- the considered substance is completely mixed over the water column. This implies that a source/sink term is considered to mix instantaneously,
- the substance is considered to be conservative or subject to a first order decay,
- Fick's diffusion law can be applied, i.e. the dispersive transport is proportional to the gradient of the concentration.

If the flow passes rapidly through the sewer system, the decay will seldom be important. In general, the dissolved substances/pollutants can be modelled as conservative or with a first order decay. The decay can be used e.g. for the description of the de-oxygenation of BOD.

22.1 The Continuity Equation for the Transport of Dissolved Substances

The one-dimensional, vertically-integrated equation for the conservation of mass of a substance in solution is given as:

$$\frac{\partial(AC)}{\partial t} + \frac{\partial T}{\partial x} = -A \cdot K \cdot C + C_s \cdot q \qquad (22.1)$$

where:

C	=	the concentration (arbitrary unit),
A	=	the area of the cross-section (m^2),
T	=	the transport,
K	=	the linear decay coefficient (s^{-1}),
C_s	=	the source/sink concentration,
q	=	the lateral inflow (m^2/s),
x	=	the space co-ordinate (m),
t	=	the time co-ordinate (s).

22.2 The Advection-Dispersion Equation

The advection-dispersion equation reflects two transport mechanisms:

- the advective transport of the dissolved substances with the mean flow velocity,
- the dispersive transport due to concentration gradients of the dissolved substance in the water.

The dispersion again reflects several phenomena, i.e. molecular diffusion, turbulent diffusion and the effect from the non-uniform velocity distribution over the cross-section.

The two first mentioned diffusion processes are rather insignificant compared to the effect from the non-uniform velocity distribution. The dispersion coefficient for the turbulent flow in a full running pipe was found through theoretical analysis by Taylor in 1954 to be:

$$k_x = \frac{D}{u_f \cdot R} = 20.2 \tag{22.2}$$

where:

k_x	=	the dimensionless dispersion coefficient,
D	=	the dispersion coefficient (m^2/s),
u_f	=	the friction velocity (m/s),
R	=	the hydraulic radius (m).

The theoretical analysis by Taylor was verified against experimental data. For a 1-meter pipe with a slope of 1.0E-2 the dispersion coefficient D is:

$$D = 20.2 \cdot \sqrt{gRI} \cdot R = 20.2\sqrt{9.81 \cdot 0.25 \cdot 1.0\mathrm{E}-2} \cdot 0.25 = 0.8 m^2/s \tag{22.3}$$

The effect of the dispersion term is probably small for sewer systems with high flow velocities, but it may become important in systems with small gradients and backwater effects. The one-dimensional vertically integrated equation for the conservation of mass of a substance in solution, i.e. the one dimensional advection-dispersion equation reads:

$$\frac{\partial(AC)}{\partial t} + \frac{\partial(QC)}{\partial x} - \frac{\partial}{\partial x}\left(AD\frac{\partial C}{\partial x}\right) = -A \cdot K \cdot C + C_c \cdot q \tag{22.4}$$

In the present numerical model, a more general description of the dispersion coefficient has been implemented. The dispersion coefficient is determined as a function of the mean flow velocity:

$$D = a \cdot |u|^b \tag{22.5}$$

where:

u = the mean velocity (m/s),
a,b = user specified constants.

Equation (22.5) can be turned into Equation (22.2) by selecting:

$$a = 20.0\frac{\sqrt{g}}{M}R^{5/6} \qquad and \qquad b = 1 \tag{22.6}$$

22.3 Boundary Conditions for the Advection-Dispersion Equation

The advection-dispersion model needs boundary conditions at all external boundaries. At external boundaries several different boundary conditions can be applied:

- outflow from an open boundary,
- flow into an open boundary,
- closed boundary.

22.3.1 Outflow From an Open Boundary

When outflow occur, the concentration is only dependent on the concentration in the model area. The open boundary outflow condition is:

$$\frac{\partial^2 C}{\partial x^2} = 0 \tag{22.7}$$

This specifies that the gradient of the concentration with respect to the distance is constant at the outflow boundary and that the transport across the boundary is pure advection.

22.3.2 Flow Into an Open Boundary

At an open inflow boundary the concentration must be specified as function of time. If the flow direction changes an outflow boundary becomes an inflow boundary and vice versa. This scenario will typically happen when the receiving water is tidal influenced. The boundary condition then changes between the concentration in the sewer system and the concentration in the receiving water according to:

$$C = C_r + (C_s - C_r)e^{\frac{-t_{mix}}{K_{mix}}} \tag{22.8}$$

where:

C_r	=	the concentration in the receiving water,
C_s	=	the concentration in the sewer system immediately before the flow direction changed,
K_{mix}	=	a time scale (hrs^{-1}),
t_{mix}	=	the elapsed time since the flow direction changed (hrs).

Equation (22.8) reflects that the first water, which enters the sewer system has the concentration of the water which last has left the sewer before the flow reversal occurred. By selecting a small value of K_{mix}, the inflow concentration changes almost immediately to the concentration in the receiving water. On the contrary, by selecting a large K_{mix}, the inflow concentration changes very slowly from the concentration in the sewer system to the concentration in the recipient.

22.3.3 Closed Boundaries

No mass is transported across a closed boundary, hence it is characterized by $q = 0.0$ and

$$\frac{\partial C}{\partial x} = 0 \tag{22.9}$$

22.4 Solution of the Advection-Dispersion Equation at Structures and Manholes

The solution of the advection-dispersion equation has to be modified at hydraulic structures in sewer systems. The general way to describe the transport at a nodal point is to set up a local continuity equation. Further, special cases exist where the local continuity equation has to be modified, e.g. when free flow into a manhole is present. The modification to the advection-dispersion equation is described below.

22.4.1 Manholes and Structures - General Solution

At manholes a local continuity equation is applied. It is assumed that the substance in the nodal point is fully mixed over the volume. This assumption might not always be fulfilled, e.g. when flooding occurs. The continuity equation for a manhole reads:

$$\frac{\partial (V_N C_N)}{\partial t} + \sum_{i=1}^{i=kk} T = -V_N \cdot C_N \cdot K_N \tag{22.10}$$

where:

V_N = the volume of the structure (m^3/s),
C_N = the concentration in the node,
T = the transport into the node (kg/s),
K_N = the decay constant for the node,
kk = the number of connecting pipes.

The continuity equation for the water flow to and from a node can be written as:

$$\frac{\partial V_N}{\partial t} + \sum_{i=1}^{i=kk} Q = 0 \qquad (22.11)$$

where Q (m^3/s) is the discharge in the connecting branches.

The continuity equation for a nodal point, Equation (22.10), can be re-arranged by use of the continuity equation for water, Equation (22.11):

$$V_N \frac{\partial C_N}{\partial t} - C_N \sum_{i=1}^{i=kk} Q + \sum_{i=1}^{i=kk} T = -V_N \cdot C_N \cdot K_N \qquad (22.12)$$

22.4.2 Free Flow Into a Manhole

When free flow into a structure occurs, i.e. the water level in the structure is lower than the water level in the inlet pipe, the concentration in the pipe is independent of the concentration at the structure. Hence, the dispersion term in the formulation of the transport is neglected, i.e. the transport is pure advection, see Figure 22.1. The transport at a structure is now formulated as:

$$T = Q \cdot C \qquad (22.13)$$

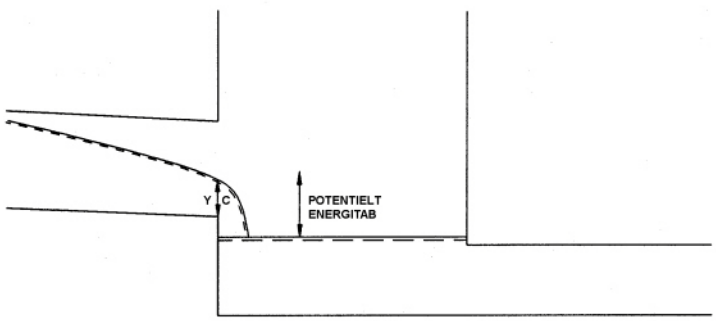

Figure 22.1 Free inflow to a manhole

22.4.3 No Outflow From a Structure to a Pipe

This condition occurs when the water level at the structure is lower than the bottom invert of the outlet pipe, see Figure 22.2. When such a situation arises, a local continuity equation is applied. The transport into the outlet pipe is described by:

$$T = Q_{pipe} \cdot C_N \tag{22.14}$$

where Q_{pipe} (m^3/s) is the discharge at the first grid point in the outlet pipe.

In reality the discharge in the outlet pipe ought to be zero. However, due to the stability of the numerical scheme in the hydrodynamic model a minimum water depth of 0.5% of the pipe diameter (maximum 0.5 cm) will always be present in the pipes. The minimum water depth is user-specified in the dhiapp.ini file. Hence, a small discharge will be present.

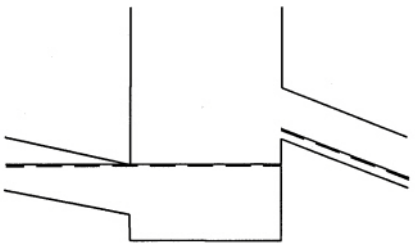

Figure 22.2 No flow from the manhole to the outlet pipe

22.5 Formulation of the Transport of Dissolved Substances Through Pumps

In general, the formulation of the transport of a dissolved substance is based on the hydrodynamic solutions of the MOUSE model. In the hydrodynamic model of MOUSE, pumps are normally described as functions between two nodes, i.e. without explicit definition of rising mains. This simplification implies instantaneous water transport and consequently, the impossibility to apply the advection-dispersion equations in such cases. The only information available is the distance between the pump and the tail node (approx. the length of the rising main) and the discharge of the pump. Hence, dissolved matter is routed through such a system with no time lag between the pump and the end of the conduit. This results in significant errors in the transport time for dissolved substances in the pipe, if the retention time of water in the conduit is much larger than the time step of the simulation. The pumped mass *qs·cs* is added to the source term of the continuity equation at the tail node.

22.6 Formulation of the Transport of Dissolved Substances Over Weirs

Transport over a weir is formulated as routing between the weir node and the destination node. The transport rate is determined on the basis of the concentration in the weir node and the weir flow. The mass flowing over the weir *qs·cs* is added to the source term of the continuity equation at the destination node.

22.7 Water Age Simulation

The development of water age is described by the advection-dispertion equation, where the first order decay term is substituted by a zero order growth term.

Thus the one-dimensional vertically integrated equation for modeling the water age is given as

$$\frac{\partial(A \cdot S)}{\partial t} + \frac{\partial(T)}{\partial x} = A + S_s \cdot q \qquad (22.15)$$

where

S	=	the age of the water
A	=	the cross section
T	=	the transport of the water that uses S
Q	=	the flow of the water
S_S	=	the age of any source/sink
q	=	the source/sink
x	=	the coefficient
t	=	the time

All equations described in previous sections 21.1 to 22.6 are also valid for the special version of the advection-dispertion equation, except that the first order decay term must be substituted by the zero order growth term.

23 The Numerical Solution for the Advection-Dispersion Model

23.1 Numerical Scheme

The advection-dispersion equation is solved using an implicit finite-difference scheme, which is centred in time and space in order to avoid the numerical dispersion. The concentrations are defined in each grid point, i.e. the grid is a non-staggered grid. A third-order correction term has been included in order to eliminate the third-order truncation error. A sketch of the numerical scheme is shown in Figure 23.1.

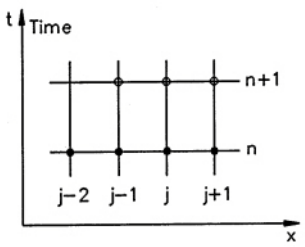

Figure 23.1 The numerical scheme for the advection-dispersion

The two equations considered are the continuity equation and the advection-dispersion equation. The continuity equation is given in Equation (22.1). A sketch of the transport of dissolved substances through a small element of water is shown in Figure 23.2.

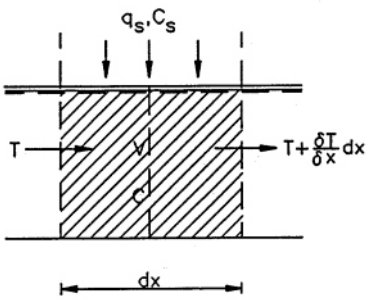

Figure 23.2 Sketch of the transport of dissolved substances through a small element of water

The continuity equation can be written in discrete form as given below:

$$\frac{(V_j C_j)^{n+1} - (V_j C_j)^n}{\Delta t} + T_{j+1/2}^{n+1/2} - T_{j-1/2}^{n+1/2} = Q_s^{n+1/2} C_s^{n+1/2} - K C_j^{n+1/2} V_j^{n+1/2} \quad (23.1)$$

where:

T	=	the transport through the box walls,
j	=	the grid point number,
n	=	the time level.

The advection-dispersion equation is given below in discrete form:

$$T_{j+1/2}^{n+1/2} = Q_{j+1/2}^{n+1/2} C_{j+1/2}^{*} - A_{j+1/2}^{n+1/2} D_{j+1/2}^{n+1/2} \frac{C_{j+1}^{n+1/2} - C_j^{n+1/2}}{\Delta x} \quad (23.2)$$

where:

$Q_{j+1/2}^{n+1/2}$	=	the discharge at the right wall of the box (m^3/s),
$A_{j+1/2}^{n+1/2}$	=	the cross sectional area of the right wall (m^2),
$D_{j+1/2}^{n+1/2}$	=	the dispersion coefficient (m^2/s) given by Equation (23.3),
$C_{j+1/2}^{*}$	=	an upstream interpolated concentration given by Equations (23.52) and (23.53).

The dispersion coefficient is calculated as:

$$D_{j+1/2}^{n+1/2} = a \cdot \left| \frac{Q_{j+1/2}^{n+1/2}}{A_{j+1/2}^{n+1/2}} \right|^b \quad (23.3)$$

where a and b are constants.

23.2 Discretization of the Boundary Conditions

23.2.1 Outflow From an Open Boundary

The open outflow boundary condition is given by Equation (22.7). The discrete form of Equation (22.7) is:

$$\frac{(V_N C_N)^{n+1} - (V_N C_N)^n}{\Delta t} + (\Delta T)^{n+1/2} = Q_s^{n+1/2} C_s^{n+1/2} - K_N C_N^{n+1/2} V_N^{n+1/2} \quad (23.4)$$

where $\Delta T^{n+1/2}$ is the transport given as:

$$\Delta T^{n+1/2} = Q_{j-1/2}^{n+1/2} C_{j-1/2}^{*} - Q_N^{n+1/2} C_N^{n+1/2} \quad (23.5)$$

23.2.2 Flow Into an Open Boundary

The discrete form of the inflow boundary condition is:

$$C_N^{n+1/2} = C_B^{n+1/2} \quad (23.6)$$

where C_B is the concentration at the boundary. If a flow reversal occurs at the boundary the outflow boundary changes to an inflow boundary and the boundary condition is given as in Equation (22.8). The discrete form of Equation (22.8) is:

$$C_N^{n+1/2} = C_r^{n+1/2} + (C_s^{n+1/2} - C_r^{n+1/2}) e^{\frac{-t_{mix}}{K_{mix}}} \quad (23.7)$$

23.2.3 Closed Boundaries

The closed boundary condition is given in Equation (22.9). The discrete form for the closed boundary is equivalent to the discrete form of the continuity equation for a manhole, which is given in the next section.

23.3 Discretization at Manholes and Structures

The continuity equation around manholes and structures, Equation (22.10), is given in the discrete form below:

$$V_N^{n+1/2}\frac{C_N^{n+1}-C_N^n}{\Delta t}+1/2(C_N^{n+1}+C_N^n)\frac{\partial V_N}{\partial t}+\sum_{k=1}^{k=kk}T \qquad (23.8)$$

$$=Q_sC_s-1/2KV_N^{n+1/2}(C_N^n+C_{N+1}^n)$$

The transport T to and from the node is given as:

$$T=1/4Q_{j+1/2}^{n+1/2}(C_N^{n+1}+C_N^n+C_{N-1}^{n+1}+C_{N-1}^n) \qquad (23.9)$$

$$+A_{N-1/2}^{n+1/2}D_{N-1/2}^{n+1/2}\left[\frac{1/2(C_N^{n+1}+C_N^n)-1/2(C_{N-1}^{n+1}+C_{N-1}^n)}{1/2\Delta x}\right]$$

where *N-1* is the grid point in pipe *k* at a distance *Dx* from the node.

23.3.1 Free Flow Into a Manhole

When free inflow to the node occurs the dispersion term in the formulation of the transport is neglected. The discrete form of the transport then yields:

$$T_j^{n+1/2}=1/2Q_j^{n+1/2}(C_j^{n+1}+C_j^n) \qquad (23.10)$$

23.3.2 No Outflow From a Structure to a Pipe

When the water level in the structure is lower than the invert of the outlet pipe, a local continuity equation is applied. The discrete form of the transport into the outlet pipe is:

$$T_j^{n+1/2}=Q_j^{n+1/2}1/2(C_N^{n+1}+C_N^n) \qquad (23.11)$$

23.4 Solution of the Finite Difference Equations

Substitution and re-arrangement of the above equations give a general implicit finite difference equation which relates the concentration in three neighbouring grid points to each other at any time level as follows:

$$\alpha_jC_{j-1}^{n+1}+\beta_jC_j^{n+1}+\gamma C_{j+1}^{n+1}=\delta^n \qquad (23.12)$$

where α, β and γ are constants.

Equation (23.12) gives a tri-diagonal matrix, i.e. a system of linear equations which is solved by the “double sweep” algorithm, as described in the the pipe-flow reference manual.

23.5 The Accuracy of the Numerical Scheme

The third order Taylor series expansion is used to ensure that the scheme has a third order accuracy. Elimination of the third order truncation error makes it possible to simulate concentration profiles with steep fronts. In general, the third order terms are associated with phase errors and wiggles in the scheme while the second order terms lead to numerical diffusion. The Taylor expansions yields:

$$C_j^{n+1} = C_j^n + \Delta t\frac{\partial C_j^n}{\partial t} + \frac{\Delta t^2}{2}\frac{\partial^2 C_j^n}{\partial t^2} + \frac{\Delta t^3}{6}\frac{\partial^3 C_j^n}{\partial t^3} \tag{23.13}$$

$$C_{j-1}^n = C_j^n - \Delta x\frac{\partial C_j^n}{\partial x} + \frac{\Delta x^2}{2}\frac{\partial^2 C_j^n}{\partial x^2} + \frac{\Delta x^3}{6}\frac{\partial^3 C_j^n}{\partial x^3} \tag{23.14}$$

$$C_{j+1}^n = C_j^n + \Delta x\frac{\partial C_j^n}{\partial x} + \frac{\Delta x^2}{2}\frac{\partial^2 C_j^n}{\partial x^2} + \frac{\Delta x^3}{6}\frac{\partial^3 C_j^n}{\partial x^3} \tag{23.15}$$

$$C_{j-2}^n = C_j^n - 2\Delta x\frac{\partial C_j^n}{\partial x} + \frac{(2\Delta x)^2}{2}\frac{\partial^2 C_j^n}{\partial x^2} + -\frac{(2\Delta x)^3}{6}\frac{\partial^3 C_j^n}{\partial x^3} \tag{23.16}$$

$$\begin{aligned} C_{j+1}^{n+1} &= C_j^n + \Delta t\frac{\partial C_j^n}{\partial t} + \Delta x\frac{\partial C_j^n}{\partial x} + \frac{\Delta t^2}{2}\frac{\partial^2 C_j^n}{\partial t^2} + \frac{\partial x^2}{2}\frac{\partial^2 C_j^n}{\partial x^2} \\ &+ \frac{2\Delta x\Delta t}{2}\frac{\partial^2 C_j^n}{\partial x\partial t} + \frac{\Delta t^3}{6}\frac{\partial^3 C_j^n}{\partial t^3} + \frac{\Delta x^3}{6}\frac{\partial^3 C_j^n}{\partial x^3} + \frac{3\Delta x^2\Delta t}{6}\frac{\partial^3 C_j^n}{\partial x^2\partial t} + \frac{3\Delta x\Delta t^2}{6}\frac{\partial^3 C_j^n}{\partial x\partial t^2} \end{aligned} \tag{23.17}$$

$$\begin{aligned} C_{j-1}^{n+1} &= C_j^n + \Delta t\frac{\partial C_j^n}{\partial t} - \Delta x\frac{\partial C_j^n}{\partial x} \\ &+ 1/2\left\{\Delta t^2\frac{\partial^2 C_j^n}{\partial t^2} + \Delta x^2\frac{\partial^2 C_j^n}{\partial x^2} - 2\Delta x\Delta t\frac{\partial^2 C_j^n}{\partial x\partial t}\right\} \\ &+ 1/6\left\{\Delta t^3\frac{\partial^3 C_j^n}{\partial t^3} - \Delta x^3\frac{\partial^3 C_j^n}{\partial x^3} + 3\Delta x^2\Delta t\frac{\partial^3 C_j^n}{\partial x^2\partial t} - 3\Delta x\Delta t^2\frac{\partial^3 C_j^n}{\partial x\partial t^2}\right\} \end{aligned} \tag{23.18}$$

By assuming that the velocity is constant locally, the second and third order derivatives in Equations (23.13) to (23.18) can be transformed to a more convenient form. The transformations used are:

$$\frac{\partial C}{\partial t} = -u\frac{\partial C}{\partial x} \tag{23.19}$$

$$\frac{\partial^2 C}{\partial x \partial t} = -u\frac{\partial^2 C}{\partial x^2} \tag{23.20}$$

$$\frac{1}{u^2}\frac{\partial^3 C}{\partial x \partial t^2} = \frac{\partial^3 C}{\partial x^3} \tag{23.21}$$

$$\frac{\partial^3 C}{\partial x^2 \partial t} = -\frac{1}{u}\frac{\partial^3 C}{\partial x \partial t^2} \tag{23.22}$$

$$\frac{\partial^3 C}{\partial t^3} = -u\frac{\partial^3 C}{\partial x \partial t^2} \tag{23.23}$$

Equation (23.19) can be turned into the general formulation:

$$\frac{\partial^n C}{\partial t^n} = (-u)^n \frac{\partial^n C}{\partial x^n} \tag{23.24}$$

The results of the Taylor expansions are inserted in the advection dispersion equation, e.g. Equation (23.13) is rewritten as:

$$C_j^{n+1} = C_j^n + \Delta t\frac{\partial C_j^n}{\partial t} + \frac{\Delta t^2}{2}u^2\frac{\partial^2 C_j^n}{\partial x^2} - \frac{\Delta t^3}{6}u^3\frac{\partial^3 C_j^n}{\partial x^3} \tag{23.25}$$

The explicit third order correction term can be found from the solution to four equations with four variables. The solution to the equations is:

$$-1/6\left(1 + \frac{\delta^2}{2}\right)\left(c_{j-2}^n - 3c_{j-1}^n + 3c_j^n - c_{j+1}^n\right) = 0 \tag{23.26}$$

where δ is the convective Courant number defined in Equation (23.54).

23.6 The Stability of the Numerical Scheme

23.6.1 Linear Stability Analysis of the Numerical Scheme

The stability of the advection equation is evaluated by applying the von Neumann condition for stability. The stability criteria is only evaluated for the advection and not for the advection-dispersion equation, since the case with pure advection sets the strongest stability criteria. The advection equation is given below:

$$\frac{\partial c}{\partial t} + u\frac{\partial c}{\partial x} = 0 \tag{23.27}$$

The analytical solution to Equation (23.27) is:

$$c(x,t) = c_0\cos(k(x-ut),0) = \sum_{j=1}^{\infty} c_j\cos\{kj(x-ut)\} \tag{23.28}$$

The harmonic solution to Equation (23.27) is:

$$c(x,t) = c_0\cos\{k(x-ut)\} = Re[c_0 e^{ik(x-ut)}] \tag{23.29}$$

where:

$x = j \cdot Dx,$
$t = n \cdot Dt.$

The numerical harmonic solution to Equation (23.27) can be written as:

$$c(x = j\Delta x, t = n\Delta t) = c_0\rho^n e^{ikj\Delta x} \tag{23.30}$$

If the analytical equation is equal to the numerical solution the following equation has to be fulfilled:

$$\rho = e^{-iku\Delta t} \tag{23.31}$$

The concentration in grid point j at time level n can now be written as:

$$c_j^n = c_0\rho^n e^{ij\xi} \tag{23.32}$$

with:

$$\xi = \Delta x \cdot k = 2\pi \frac{\Delta x}{L} \tag{23.33}$$

The von Neumann stability condition is based on a linear stability analysis in which it is assumed that the solution to the finite difference scheme can be written as a Fourier series in complex, exponential form for any time level, *n*, in the form:

$$c_j^n = \sum_{k=1}^{k=kk} \rho_k^n e^{ik\alpha_j} \qquad k = 1, 2, 3, ..., kk \tag{23.34}$$

where:

α = the dimensionless wave number,
k = a finite index.

The linear stability analysis determines how the Fourier coefficients behave in time for a fixed wave number. The concentration at grid point *j* at time *n* for the wave number *k* = 1, can be written as:

$$c_j^n = c_0 \rho^n e^{ij\xi} \tag{23.35}$$

In a similar way, the concentration at grid point *j* at time level *n+1* and the concentration at grid point *j+1* at time level *n* can be written as:

$$c_j^{n+1} = \rho^{n+1} e^{i\alpha j} \tag{23.36}$$

and

$$c_{j+1}^n = \rho^n e^{i\alpha(j+1)} \tag{23.37}$$

23.6.2 The Stability of the Advection Equation

The one-dimensional advection equation is given by:

$$\frac{\partial c}{\partial t} = u \frac{\partial c}{\partial x} \tag{23.38}$$

The discretization of the one-dimensional advection equation, accurate to the third order, is given by:

$$\frac{c_j^{n+1} - c_j^n}{\Delta t} = u\frac{c_{j+½}^{n+½} + (c_{j+1}^n - 2c_j^n + c_{j-1}^n) - c_{j-½}^{n+½} - (c_j - 2c_{j-1} + c_{j-2})}{\Delta x} \quad (23.39)$$

Equation (23.39) is transformed to complex numbers by using the following substitutions:

$$c_j^{n+½} = 1/2(c_j^{n+1} + c_j^n) = \frac{\rho + 1}{2}c_j^n \quad (23.40)$$

$$\frac{c_{j+1}^n - c_{j-1}^n}{2} \cdot \frac{1}{c_j^n} = \frac{e^{i\xi} - e^{-i\xi}}{2} = i\sin\xi \quad (23.41)$$

$$c_{j+½}^{n+½} - c_{j-½}^{n+½} = c_j^n\frac{1+\rho}{2}\left(e^{\frac{i\xi}{2}} - e^{\frac{-i\xi}{2}}\right) = c_j^n\frac{1+\rho}{2} \cdot 2i\sin\left(\frac{\xi}{2}\right) \quad (23.42)$$

$$c_{j+1}^n - 2c_j^n + c_{j-1}^n = \rho^n e^{i\xi} - 2\rho^n + \rho^n e^{-i\xi} = \rho^n(-2 + 2\cos\xi) \quad (23.43)$$

$$c_j^n - 2c_{j-1}^n + c_{j-2}^n = \rho^n - 2\rho^n e^{-i\xi} + \rho^n e^{-2i\xi} = e^{-i\xi}\rho^n(-2 + 2\cos\xi) \quad (23.44)$$

Using the Equations (23.40) to (23.44), the equation (23.39) can be written as:

$$\rho^{n+1} - \rho^n = \sigma[\rho^n ½(1+\rho)i\sin\xi - \rho^n(-2 + 2\cos\xi) \cdot (1 - \cos\xi + i\sin\xi)] \quad (23.45)$$

where σ is the Courant number ($u \cdot Dt/Dx$).

Short waves:

For the shortest resolvable wave (the Nyquist frequency) the wave length, L, is given as:

$$L = 2\pi \Rightarrow \xi = \pi \quad (23.46)$$

i.e.

$$\sin\xi = 0 \qquad \cos\xi = -1$$

Equation (23.45) now gives:

$$\rho^{n+1} = \beta\rho^n(1 - 8\sigma) \quad (23.47)$$

where ($1 - 8s$) is the amplification factor E.

The stability criterion is:

$$|E| \leq 1 \tag{23.48}$$

The solution to Equation (23.48) is:

$$\beta = \frac{1}{4\sigma} \tag{23.49}$$

Long waves:

For the longest the wave length, *L*, is given as:

$$L = 2\pi \Rightarrow \xi\_0, \tag{23.50}$$

i.e.

$$\sin\xi = \xi \qquad \cos\xi = 1 - \frac{\xi^2}{2}$$

Equation (23.45) now gives:

$$\rho^{n+1} - \rho^n = \sigma\left[p^n \frac{1+\rho}{2} i\xi - \rho^n\left(-2 + 2\left(1 - \frac{\xi^2}{2}\right)\right) \cdot \left(1 - \left(1 - \frac{\xi^2}{2}\right) + i\xi\right)\right] \tag{23.51}$$

The approximation to the upstream-interpolated concentration can now be given as:

If $\sigma < 1$ then:

$$C^*_{j+\frac{1}{2}} = \frac{1}{4}(C^{n+1}_{j+1} + C^{n+1}_j + C^n_{j+1} + C^n_j) - \frac{1}{6}\left(1 + \frac{\sigma^2}{2}\right) \cdot (C^n_{j+1} - 2C^n_j + C^n_{j-1}) \tag{23.52}$$

If $\sigma \geq 1$ then

$$C^*_{j+\frac{1}{2}} = \frac{1}{4}(C^{n+1}_{j+1} + C^{n+1}_j + C^n_{j+1} + C^n_j) \tag{23.53}$$

The phase and the amplitude portraits of the numerical scheme are shown in Figure 23.3 and Figure 23.4.

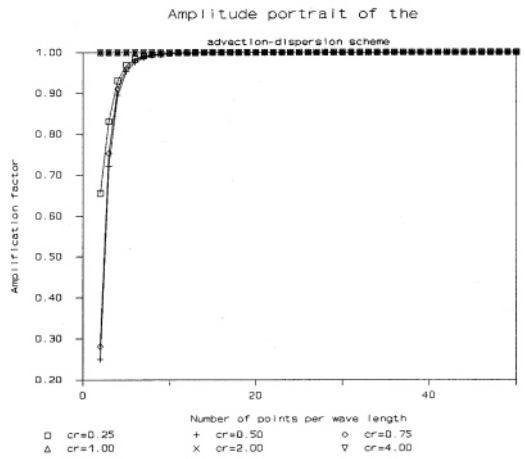

Figure 23.3 The amplitude portrait of the advection-dispersion scheme

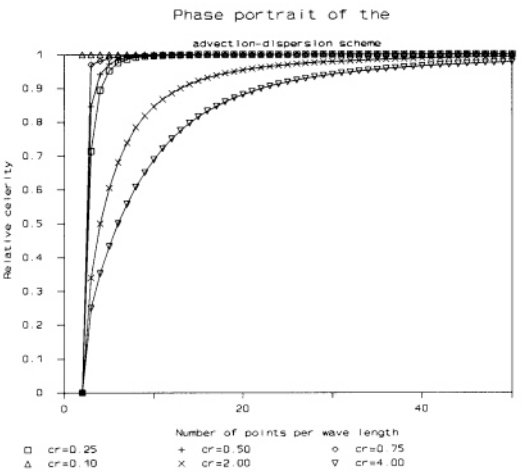

Figure 23.4 The phase portrait of the advection-dispersion scheme

Even if the scheme is stable there are some restrictions on the selection of the time step, Δt, and the grid size, Δx. The stability criterion is expressed in terms of the convective Courant number, defined as:

$$\delta = \frac{|u| \cdot \Delta t}{\Delta x} \tag{23.54}$$

The stability criterion is:

$$C_c = \frac{|u| \cdot \Delta t}{\Delta x} < 1 \tag{23.54a}$$

Another dimensionless number used to describe the numerical scheme is the Peclet number. This is defined as:

$$Pe = \frac{|u| \cdot \Delta x}{D} \tag{23.55}$$

The numerical scheme is stable even for large Peclet numbers, i.e. $Pe > 2$. However, the Peclet number is associated with numerical oscillations, wiggles, which grow or decay spatially with a wave length of $2\Delta x$. In a diffusion-free scheme which is stable in the von Neumann, wiggles are likely to occur when large gradients in the concentration are present. The criterion for the absence of wiggles is:

$$Pe \leq 2 \tag{23.56}$$

The wiggles can be eliminated from the numerical scheme by an upstream centring of the numerical scheme, which introduces numerical diffusion into the scheme or by use of the *n-1* time step in the computations.

24 Nomenclature

A	cross-sectional area (m^2),
a	constant in Equation (23.3),
b	constant in Equation (23.3),
c	concentration (arbitrary unit),
c_r	boundary concentrations,
c_N	concentration in the node,
c_q	concentration of lateral inflow source,
c_s	concentration at the boundary immediately before the flow direction changed,
c_s	source/sink concentration,
D	dispersion coefficient (m^2/s),
E	amplification factor,
j	grid point number,
K	linear decay coefficient (s^{-1}),
K_{mix}	a time scale ($hours^{-1}$),
K_N	decay constant for the node (s^{-1}),
kk	number of connecting pipes,
k_x	dimensionless dispersion coefficient,
n	time level,
Pe	the Peclet number,
Q	discharge (m^3/s),
Q_{pipe}	discharge at the first grid point in the outlet pipe, (m^3/s)
q	discharge per unit width (m^2/s),
R	hydraulic radius (m),
T	transport through box walls,
t	time coordinate (s),
t_{mix}	time passed since the flow direction changed (s),
u	mean velocity (m/s),
u_f	friction velocity (m/s),
V	volume (m^3/s),
V_N	volume of the structure (m^3/s),
x	space coordinate (m),
α	constant in Equation (23.12),
β	constant in Equation (23.12),
γ	constant in Equation (23.12),
d	convective Courant number.

25 References

/1/Abbot, M. B., “Computational Hydraulics, Elements of the Theory of Free Surface Flow”. Pitman Publishing Limited, London, 1985.

/2/Abbot, M. B., Basco, D.R., “Computational Fluid Dynamics, An Introduction for Engineers”. Longman Scientific & Technical, England 1989.

/3/Ames, W. F., “Numerical Methods for Partial Differential Equations”. ACADEMIC PRESS, INC, New York 1977.

/4/Cunge, J.A., Holly. F.M., Verwey, A. “ Practical Aspects of Computational River Hydraulics”, Pitman Publishing Limited, London, 1980.

/5/Kluesener, J.W and Lee, G.F., “Nutrient Loading from a Separate Sewer in Madison, Wisconsin,” Journal Water Pollution Contol Federation, pp. 920-936, Vol. 46, No. 5, May 1974.

/6/Mattaw, H.C., Jr., and Sherwood, C.B., “Quality of Storm Water Runoff From a Residential Area, Broward County, Florida,” Journal Research U.S. Geological Survey, pp. 832-834, Vol. 5, No. 6, 1977.